



A finite element based fast eigensolver for three dimensional anisotropic photonic crystals

So-Hsiang Chou^{a,*}, Tsung-Ming Huang^{b,*}, Tiexiang Li^c, Jia-Wei Lin^d,
Wen-Wei Lin^d

^a Department of Mathematics and Statistics, Bowling Green State University, OH, USA

^b Department of Mathematics, National Taiwan Normal University, Taipei 116, Taiwan

^c School of Mathematics, Southeast University, Nanjing 211189, People's Republic of China

^d Department of Applied Mathematics, National Chiao Tung University, Hsinchu 300, Taiwan



ARTICLE INFO

Article history:

Received 17 December 2017

Received in revised form 3 January 2019

Accepted 5 February 2019

Available online 4 March 2019

Keywords:

Maxwell's equations

Three-dimensional anisotropic photonic crystals

Face-centered cubic lattice

Finite element method

Null-space free eigenvalue problem and fast Fourier transforms

ABSTRACT

The standard Yee's scheme for the Maxwell eigenvalue problem places the discrete electric field variable at the midpoints of the edges of the grid cells. It performs well when the permittivity is a scalar field. However, when the permittivity is a Hermitian full tensor field it would generate un-physical complex eigenvalues or frequencies. In this paper, we propose a finite element method which can be interpreted as a modified Yee's scheme to overcome this difficulty. This interpretation enables us to create a fast FFT eigensolver that can compute very effectively the band structure of the anisotropic photonic crystal with SC and FCC lattices. Furthermore, we overcome the usual large null space associated with the Maxwell eigenvalue problem by deriving a null-space free discrete eigenvalue problem which involves a crucial Hermitian positive definite linear system to be solved in each of the iteration steps. It is demonstrated that the CG method without preconditioning converges in 37 iterations even when the dimension of a matrix is as large as 5, 184, 000.

© 2019 Elsevier Inc. All rights reserved.

1. Introduction

In this paper we are concerned with a fast numerical eigensolver for the Maxwell eigenvalue problem

$$\nabla \times \nabla \times \mathbb{E} = \lambda \varepsilon \mathbb{E}, \quad \lambda = \mu \omega^2, \quad (1a)$$

$$\nabla \cdot \varepsilon \mathbb{E} = 0 \quad (1b)$$

posed on Ω , which is a primitive cell with lattice vectors \mathbf{a}_ℓ , $\ell = 1, 2, 3$, of a periodic structure in \mathbb{R}^3 such as a photonic crystal (PC). Here in (1), $\mathbb{E} = \mathbb{E}(\mathbf{x})$ is the electric field, ε is the periodic permittivity complex tensor field, and μ is the constant permeability scalar field. Mathematically, this problem arises naturally from the source-free Maxwell equations by assuming that the time dependent electric and magnetic fields are time-harmonic with a factor of $e^{-i\omega t}$ ($i = \sqrt{-1}$). In an anisotropic medium, the permittivity ε may take a Hermitian form [27–29]

* Corresponding authors.

E-mail addresses: chou@bgsu.edu (S.-H. Chou), min@ntnu.edu.tw (T.-M. Huang), txli@seu.edu.cn (T. Li), jiawei.am05@g2.nctu.edu.tw (J.-W. Lin), wwlin@math.nctu.edu.tw (W.-W. Lin).

<https://doi.org/10.1016/j.jcp.2019.02.029>

0021-9991/© 2019 Elsevier Inc. All rights reserved.

$$\varepsilon = \begin{bmatrix} \varepsilon_{11} & \ell\varepsilon_{12} & \ell\varepsilon_{13} \\ -\ell\varepsilon_{12} & \varepsilon_{22} & \ell\varepsilon_{23} \\ -\ell\varepsilon_{13} & -\ell\varepsilon_{23} & \varepsilon_{33} \end{bmatrix}. \quad (2)$$

Anisotropic PC material has many interesting and novel applications in practice, such as the hollow semiconductor nanorod [22], femtosecond laser pulses [38], photonic crystal fibers [2,6,37], among others. In 1993, it was shown that the anisotropy of the material could split the degenerate band and narrow the band gap of a PC [41]. Later in 1998, a large band gap opening by using an anisotropic PC was shown in [23,24]. Thereafter, to exhibit large band gap tenability, a three-dimensional (3D) inverse opal PC structure infiltrated with liquid crystals was proposed in [7].

Computational methods play an equally important role in the study of the anisotropic material. The spectral element method [30], the finite-element method (FEM) [3,4,10,11,35], the mixed finite element method [21,25,26], the finite-difference frequency-domain method (FDFD) [13,36], and the plane wave expansion method [20] have been proposed to compute the band structure of the anisotropic PC. In this paper, we are interested in creating a finite element method that resembles the finite difference Yee's scheme [40] due to its robustness in solving the Maxwell eigenvalue problems associated with isotropic materials. Yee's scheme only discretizes (1a) and leaves the divergence-free condition (1b). The reason for that is formerly the exact solution of (1a) satisfies (1b). Indeed, this strategy works well for isotropic materials. Thus, when it comes to the discretization of (1a)-(1b) or its many possible weak formulations through finite difference or finite element schemes, the traditional wisdom is to use spatial discretizations that admit discrete analogue of the divergence free condition. This class of spatial discretizations includes Yee's scheme [14,16,40], the Whitney form [5,39], the covolume discretization [34], the mimetic discretization [19] and the edge element [32,33]. It should be noted that in all these cases the permittivity ε is a scalar field. In this paper, we will follow this approach, i.e., we will discretize (16a) in such a way that enables us to rigorously show in Theorem 5 of Sec. 5.2 that the discretized version of the weak divergence free condition (16b) is automatically satisfied, which is by no means a trivial task. On the other hand, there are certainly other approaches, e.g., [4] that keep (16b). They have the advantage of the availability of a general convergence theory of [3] for eigenvalue problems posed on general domains. However, for cuboid domains our approach can generate fast eigensolvers. The availability of such solvers is essential when the same large Maxwell eigenvalue problem has to be solved a large number of times when the material parameters in the constitutive relations must be varied in design problems [17].

On a 3D PC, due to the divergence-free condition (1b), a large null space of the underlying eigenvalue problem will be produced. The presence of the huge null space is a numerically challenging problem in solving the eigenvalue problem. Moreover, how to efficiently solve the associated linear system in each step of the eigensolver is another challenging problem.

In the 3D non-anisotropic cases (isotropic or bi-isotropic medium), we have had successes [8,14] in tackling these obstacles that were present when using Yee's scheme [40] in which \mathbb{E} is assigned to the edge centers and the magnetic field \mathbb{H} to the face centers. After the discretization phase, a generalized eigenvalue problem (GEP) with a large null space is produced. It is rather remarkable that a null-space free method with FFT (fast Fourier transform)-based matrix-vector multiplications has been found [8,14] to explicitly deflate this huge null space so that the GEP is transformed into a null-space free standard eigenvalue problem (NFSEP). The coefficient matrix of the NFSEP is Hermitian positive definite (HPD) and well-conditioned. Therefore, the associated linear system in each iteration of the invert Lanczos method can be efficiently solved by the conjugate gradient (CG) method without any preconditioner. In the dispersive PC with isotropic medium (i.e., ε is a piecewise nonlinear function of λ), a Newton-type iterative method [18] with the null-space free method is proposed to solve the associated nonlinear eigenvalue problem.

The successes of the null-space free method in isotropic and bi-isotropic PCs are partially due to the fact that the permittivity ε is a piecewise constant scalar field, and there is no conflict in the placement of discrete permittivity variable. In other words, it meshes well with the standard discretization by Yee's scheme. However, for the anisotropic material, there is a conflict in the placement of discrete tensor permittivity variable. How to modify Yee's scheme so that the null-space free method can be applied to a tensor field ε is one of the issues addressed in this paper.

In an anisotropic medium, the permittivity ε is given in the tensor form (2) where ε_{ij} , for $1 \leq i, j \leq 3$, are piecewise constants or piecewise nonlinear functions. Moreover, in [27,28], the tensor ε is HPD. A FDTD method [36] for modeling electromagnetic scattering is proposed to discretize the general anisotropic objects. The important structure and property of the tensor ε in (2) were not considered in this discretization. In this paper, we will exclusively consider the case in which the Hermitian matrix in (2) satisfies that ε_{ij} are piecewise constant, and propose a new finite element scheme which preserves the Hermitian and positive definiteness (if ε has) in the discretization. The main contributions in this paper are summarized as follows:

- Our new finite element method can be interpreted as a modified finite difference Yee's scheme. As a consequence, the discretization of the double curl operator in our proposed method is equivalent to the corresponding operator in Yee's scheme so that the null-space free method [8,14] can be applied to solve the resulting generalized eigenvalue problem. Furthermore, a well-known feature of the classical finite difference Yee's scheme for isotropic materials is that the divergence free condition of the field is automatically satisfied by the finite difference solution. In other words, one needs not to discretize (1b) explicitly. We show in Theorem 5 that our method preserves this feature for anisotropic materials as well.

- For the right-hand side of (1a), our method provides an HPD-preserving coefficient matrix B_ε , i.e., if ε is HPD, so is B_ε . Furthermore, the matrix B_ε can be factorized by FFT-matrices, diagonal matrices and a 3×3 block diagonal matrix with a suitable permutation. The special factorization of B_ε results in minimal effort in inverting B_ε while still keeping the correct physics intact (real frequencies).
- Based on the above important factorization of B_ε , the null-space free method can be applied to reduce the GEP into a NFSEP with HPD coefficient matrix. The NFSEP can be solved by the invert Lanczos method and the CG method without preconditioning can be used to solve the linear system efficiently at each iteration. The computational cost of the matrix-vector multiplication in the CG method is almost equal to that of the null-space free method in isotropic PCs.

This paper is organized as follows. We introduce our proposed finite element method in Section 2. The equivalence between our method and Yee’s scheme for the discretization of double-curl operator is shown in Section 3. The discretization of $\varepsilon\mathbb{E}$ is introduced in Section 4. In Section 5, we show that the coefficient matrix corresponding to ε is HPD, and the divergence free condition is automatically satisfied for the approximate electric field. Finally, the numerical efficiency of the developed schemes is studied in Section 6.

2. A finite element method for Maxwell eigenvalue problem

In this section, we propose a weak formulation for the Maxwell eigenvalue problem (1) and a Galerkin finite element method to solve it.

2.1. Weak formulation of problem (1)

Denote by (\mathbf{f}, \mathbf{g}) the complex inner product of \mathbb{C}^N -valued functions in $L^2(\Omega)$, i.e.,

$$(\mathbf{f}, \mathbf{g}) = \int_{\Omega} \sum_{i=1}^N f_i(\mathbf{x}) \overline{g_i(\mathbf{x})} d\mathbf{x} = \int_{\Omega} \mathbf{g}^*(\mathbf{x}) \mathbf{f}(\mathbf{x}) d\mathbf{x}. \tag{3}$$

Here “*” denotes the conjugate transpose. Let Ω be a primitive cell with lattice vectors $\mathbf{a}_\ell, \ell = 1, 2, 3$. It is known that the electric field satisfies the quasi-periodic condition

$$\mathbb{E}(\mathbf{x} + \mathbf{a}_\ell) = e^{i2\pi \mathbf{k} \cdot \mathbf{a}_\ell} \mathbb{E}(\mathbf{x}), \quad \ell = 1, 2, 3, \tag{4}$$

for all $\mathbf{x} \in \mathbb{R}^3$, where the Bloch wave vector \mathbf{k} lies in the first Brillouin zone \mathcal{B} .

Corresponding to \mathbb{E} , we can define a periodic function \mathbf{u} , its associated modulating amplitude, as

$$\mathbf{u}(\mathbf{x}) = e^{-i2\pi \mathbf{k} \cdot \mathbf{x}} \mathbb{E}(\mathbf{x}), \tag{5}$$

which satisfies the periodic condition

$$\mathbf{u}(\mathbf{x} + \mathbf{a}_\ell) = \mathbf{u}(\mathbf{x}), \quad \ell = 1, 2, 3. \tag{6}$$

Thus one can also study the Maxwell eigenvalue problem (1) by the equivalent system in terms of \mathbf{u} :

$$\nabla_{\mathbf{k}} \times \nabla_{\mathbf{k}} \times \mathbf{u} = \lambda \varepsilon \mathbf{u}, \tag{7a}$$

$$\nabla_{\mathbf{k}} \cdot \varepsilon \mathbf{u} = 0, \tag{7b}$$

where the shifted gradient operator $\nabla_{\mathbf{k}} := \nabla + i2\pi \mathbf{k}$.

Remark 1. This \mathbf{u} -system (7) has the advantage of having Fourier analysis at our disposal when analyzing the existence, stability, and convergence issues, see [11,35]. However, in this paper we are more concerned with creating fast eigensolvers and the \mathbb{E} -system (1) will be used. We will have occasions of interpreting some nice spectral-theory results from [35, Chapter 4] back to the \mathbb{E} -system.

We need to introduce some complex-valued function spaces. Let

$$H(\text{curl}, \Omega) := \{v : \Omega \rightarrow \mathbb{C}^3 \mid v, \nabla \times v \in L^2(\Omega)\}$$

with the norm

$$\|v\|_{H(\text{curl}, \Omega)}^2 := \|v\|_{L^2(\Omega)}^2 + \|\nabla \times v\|_{L^2(\Omega)}^2,$$

and let

$$\mathbf{C}_{\text{per}}^{\infty}(\Omega) := \{\phi|_{\Omega} : \phi : \mathbb{R}^3 \rightarrow \mathbb{C}, \phi \in C^{\infty}(\mathbb{R}^3), \phi(\mathbf{x} + \mathbf{a}_{\ell}) = \phi(\mathbf{x}), \ell = 1, 2, 3\},$$

$$\mathbf{C}_{\text{per}}^{\infty}(\Omega) := \{v|_{\Omega} : v : \mathbb{R}^3 \rightarrow \mathbb{C}^3, v \in C^{\infty}(\mathbb{R}^3), v(\mathbf{x} + \mathbf{a}_{\ell}) = v(\mathbf{x}), \ell = 1, 2, 3\}.$$

Define the periodic function spaces

$$H_{\text{per}}(\text{curl}, \Omega) := \text{the closure of } \mathbf{C}_{\text{per}}^{\infty}(\Omega) \text{ in } H(\text{curl}, \Omega), \quad (8a)$$

$$H_{\text{per}}^1(\Omega) := \text{the closure of } C_{\text{per}}^{\infty}(\Omega) \text{ in } H^1(\Omega), \quad (8b)$$

and their associated quasi-periodic function spaces

$$H_{\text{qper}}(\text{curl}, \Omega) := \{v : e^{-i2\pi\mathbf{k}\cdot\mathbf{x}}v \in H_{\text{per}}(\text{curl}, \Omega)\}, \quad (8c)$$

$$H_{\text{qper}}^1(\Omega) := \{\phi : e^{-i2\pi\mathbf{k}\cdot\mathbf{x}}\phi \in H_{\text{per}}^1(\Omega)\}. \quad (8d)$$

Note that in view of (5), (6) and the Fourier series representation, functions in the above two spaces satisfy the quasi-periodic conditions (4).

Theorem 1. For any $\mathbb{E}, \mathbb{W} \in C^{\infty}(\mathbb{R}^3) \cap H_{\text{qper}}(\text{curl}, \Omega)$ and $\phi \in C^{\infty}(\mathbb{R}^3) \cap H_{\text{qper}}^1(\Omega)$, we have

$$(\nabla \times \nabla \times \mathbb{E}, \mathbb{W}) = (\nabla \times \mathbb{E}, \nabla \times \mathbb{W}), \quad (9a)$$

$$(\nabla(\varepsilon\mathbb{E}), \phi) = (\varepsilon\mathbb{E}, \nabla\phi). \quad (9b)$$

Proof. Since \mathbb{E} and \mathbb{W} are smooth, Green's formula implies

$$(\nabla \times \nabla \times \mathbb{E}, \mathbb{W}) = (\nabla \times \mathbb{E}, \nabla \times \mathbb{W}) + \int_{\partial\Omega} \nu \times \nabla \times \mathbb{E} \cdot \overline{\mathbb{W}} dA, \quad (10)$$

where ν is the outward unit normal vector to the boundary. For convenience, we name the six boundary surfaces of the primitive cell Ω as $\partial\Omega_{\mathbf{a}_1}^0$, $\partial\Omega_{\mathbf{a}_1}^1$, $\partial\Omega_{\mathbf{a}_2}^0$, $\partial\Omega_{\mathbf{a}_2}^1$, $\partial\Omega_{\mathbf{a}_3}^0$ and $\partial\Omega_{\mathbf{a}_3}^1$, where

$$\partial\Omega_{\mathbf{a}_1}^s = \{s\mathbf{a}_1 + a\mathbf{a}_2 + b\mathbf{a}_3 \mid a, b \in [0, 1]\},$$

$$\partial\Omega_{\mathbf{a}_2}^s = \{s\mathbf{a}_2 + a\mathbf{a}_3 + b\mathbf{a}_1 \mid a, b \in [0, 1]\},$$

$$\partial\Omega_{\mathbf{a}_3}^s = \{s\mathbf{a}_3 + a\mathbf{a}_1 + b\mathbf{a}_2 \mid a, b \in [0, 1]\},$$

for $s = 0, 1$. Then the surface integral term in (10) can be divided as

$$\sum_{\ell=1}^3 \left(\int_{\partial\Omega_{\mathbf{a}_{\ell}}^0} \nu_{\ell,0} \times \nabla \times \mathbb{E} \cdot \overline{\mathbb{W}} dA + \int_{\partial\Omega_{\mathbf{a}_{\ell}}^1} \nu_{\ell,1} \times \nabla \times \mathbb{E} \cdot \overline{\mathbb{W}} dA \right)$$

where $\nu_{\ell,0} = -\nu_{\ell,1}$ are the outward unit normal vectors on $\partial\Omega_{\mathbf{a}_{\ell}}^0$ and $\partial\Omega_{\mathbf{a}_{\ell}}^1$, respectively. In particular, from the quasi-periodicity of \mathbb{E} and \mathbb{W} , we have

$$\begin{aligned} \int_{\partial\Omega_{\mathbf{a}_{\ell}}^0} \nu_{\ell,0} \times \nabla \times \mathbb{E}(\mathbf{x}) \cdot \overline{\mathbb{W}}(\mathbf{x}) dA &= \int_{\partial\Omega_{\mathbf{a}_{\ell}}^0} \nu_{\ell,0} \times \nabla \times \mathbb{E}(\mathbf{x} + \mathbf{a}_{\ell}) \cdot \overline{\mathbb{W}}(\mathbf{x} + \mathbf{a}_{\ell}) dA \\ &= \int_{\partial\Omega_{\mathbf{a}_{\ell}}^1} -\nu_{\ell,1} \times \nabla \times \mathbb{E}(\mathbf{x}) \cdot \overline{\mathbb{W}}(\mathbf{x}) dA, \end{aligned}$$

for $\ell = 1, 2, 3$. Therefore, the result in (9a) is proved.

To show (9b), we observe that

$$(\nabla \cdot \varepsilon\mathbb{E}, \phi) = (\varepsilon\mathbb{E}, -\nabla\phi) + \int_{\partial\Omega} \varepsilon\mathbb{E} \cdot \nu \overline{\phi} dA. \quad (11)$$

Again, the surface integral term in (11) can be divided as

$$\sum_{\ell=1}^3 \left(\int_{\partial\Omega_{\mathbf{a}_\ell}^0} \varepsilon \mathbb{E} \cdot \nu_{\ell,0} \overline{\phi} dA + \int_{\partial\Omega_{\mathbf{a}_\ell}^1} \varepsilon \mathbb{E} \cdot \nu_{\ell,1} \overline{\phi} dA \right).$$

From the periodicity of ε , and the quasi-periodicity of \mathbb{E} and ϕ , we have

$$\begin{aligned} \int_{\partial\Omega_{\mathbf{a}_\ell}^0} \varepsilon \mathbb{E}(\mathbf{x}) \cdot \nu_{\ell,0} \overline{\phi(\mathbf{x})} dA &= \int_{\partial\Omega_{\mathbf{a}_\ell}^0} \varepsilon(\mathbf{x} + \mathbf{a}_\ell) \mathbb{E}(\mathbf{x} + \mathbf{a}_\ell) \cdot \nu_{\ell,0} \overline{\phi(\mathbf{x} + \mathbf{a}_\ell)} dA \\ &= \int_{\partial\Omega_{\mathbf{a}_\ell}^1} \varepsilon(\mathbf{x}) \mathbb{E}(\mathbf{x}) \cdot (-\nu_{\ell,1}) \overline{\phi(\mathbf{x})} dA \end{aligned}$$

for $\ell = 1, 2, 3$. The result in (9b) is obtained. \square

In view of Theorem 1, a simple density argument suggests that we consider the following weak formulation of problem (1): Find a pair (λ, \mathbb{E}) with $\lambda \in \mathbb{C}$ and $\mathbb{E} \in H_{\text{qper}}(\text{curl}, \Omega)$ such that

$$(\nabla \times \mathbb{E}, \nabla \times \mathbb{W}) = \lambda(\varepsilon \mathbb{E}, \mathbb{W}), \quad \forall \mathbb{W} \in H_{\text{qper}}(\text{curl}, \Omega), \tag{12a}$$

$$(\varepsilon \mathbb{E}, \nabla \phi) = 0, \quad \forall \phi \in H_{\text{qper}}(\Omega). \tag{12b}$$

However, from a computational electromagnetics viewpoint, it is more convenient to work with the following two spaces whose description is more accessible: For functions $u : \mathbb{R}^3 \rightarrow \mathbb{C}^3$ and $\phi : \mathbb{R}^3 \rightarrow \mathbb{C}$, we define

$$H_{\text{curl}}(\Omega) = \{u|_\Omega : u \in H(\text{curl}, \Omega), u(\mathbf{x} + \mathbf{a}_\ell) = e^{i2\pi \mathbf{k} \cdot \mathbf{a}_\ell} u(\mathbf{x}), \ell = 1, 2, 3\}, \tag{13}$$

$$H_{\text{grad}}(\Omega) = \{\phi|_\Omega : \phi \in H^1(\Omega), \phi(\mathbf{x} + \mathbf{a}_\ell) = e^{i2\pi \mathbf{k} \cdot \mathbf{a}_\ell} \phi(\mathbf{x}), \ell = 1, 2, 3\}. \tag{14}$$

Remark 2. Alternatively, the quasi-periodic condition in (13) can be viewed as a way to extend the functions outside of Ω , while the regularity condition $u \in H(\text{curl}, \Omega)$, together with the quasi-periodic condition, implies a tangential boundary (trace) condition on $\partial\Omega$:

$$u_T(\mathbf{x} + \mathbf{a}_\ell) = e^{i2\pi \mathbf{k} \cdot \mathbf{a}_\ell} u_T(\mathbf{x}), \ell = 1, 2, 3, \tag{15}$$

where $u_T = \nu \times u$ is the tangential trace of u .

In fact, $H_{\text{grad}}(\Omega) = H_{\text{qper}}^1(\Omega)$ and $H_{\text{curl}}(\Omega) = H_{\text{qper}}(\text{curl}, \Omega)$. It is not hard to see that the first relation holds. The proof of the second relation and (15) uses similar arguments in proving two characterizations of $H_0(\text{curl})$ are equivalent (cf. [31, Theorem 3.33] or [12, Theorem 2.12]). See also [1, Lemma 2.1]. The analogy is not surprising, if we view the difference of (15) as a zero-trace condition.

In summary, we shall consider the weak formulation of problem (1): Find a pair (λ, \mathbb{E}) with $\lambda \in \mathbb{C}$ and $\mathbb{E} \in H_{\text{curl}}(\Omega)$ such that

$$(\nabla \times \mathbb{E}, \nabla \times \mathbb{W}) = \lambda(\varepsilon \mathbb{E}, \mathbb{W}), \quad \forall \mathbb{W} \in H_{\text{curl}}(\Omega), \tag{16a}$$

$$(\varepsilon \mathbb{E}, \nabla \phi) = 0, \quad \forall \phi \in H_{\text{grad}}(\Omega), \tag{16b}$$

where $\varepsilon : \mathbb{R}^3 \rightarrow \mathbb{C}^{3 \times 3}$ is a tensor field of the general form (not necessarily Hermitian)

$$\varepsilon = \begin{bmatrix} \varepsilon_{11} & \varepsilon_{12} & \varepsilon_{13} \\ \varepsilon_{21} & \varepsilon_{22} & \varepsilon_{23} \\ \varepsilon_{31} & \varepsilon_{32} & \varepsilon_{33} \end{bmatrix}. \tag{17}$$

Remark 3. Due to the existence of an exact de Rham sequence (cf. [35, p. 58]) and Remark 1, it implies that

$$\nabla(H_{\text{grad}}(\Omega)) \subset H_{\text{curl}}(\Omega). \tag{18}$$

Thus we can set $\mathbb{W} = \nabla \phi$ in (16a) and see that [9] when $\lambda \neq 0$, the divergence free condition is automatically satisfied. Our discrete weak formulation below will respect this property (see subsection 5.2):

$$\nabla(H_{\text{grad}}^h(\Omega)) \subset H_{\text{curl}}^h(\Omega). \tag{19}$$

Remark 4. It may be curious that why there is no need in introducing a Lagrange multiplier in the above weak formulation. See [35, Proposition 4.20] for such a case. Using the techniques in [35] via (5), we can show a result similar to the Prop. 4.20: Suppose that ε is HPD. Then for each $\mathbf{k} \in \mathcal{B}$, first Brillouin zone, the eigenvalue problem (16) has an increasing sequence $\{\lambda_j\}_{j \in \mathbb{N}}$ of non-negative real numbers tending to infinity. Each eigenvalue has finite multiplicity and zero is an eigenvalue if and only if $\mathbf{k} = \mathbf{0}$. The details will be reported elsewhere. As a consequence, zero eigenvalue is not only nonphysical, but mathematically spurious for the $\mathbf{k} \neq \mathbf{0}$ case, when a discrete weak formulation of the Maxwell eigenvalue problem produces zero eigenvalue. A null-space free method would be called for in such a case.

2.2. Discretizations of weak formulations of (16)

In this subsection, we use a Galerkin finite element method based on the edge elements to approximate the exact field \mathbb{E} in (16a). To this end, let $H_{\text{curl}}^h(\Omega)$ and $H_{\text{grad}}^h(\Omega)$ be $3N$ -dimensional linear subspaces of $H_{\text{curl}}(\Omega)$ and N -dimensional linear subspace of $H_{\text{grad}}(\Omega)$, respectively (to be defined in (23) and (24), respectively). Then a straightforward Galerkin method for (16a)-(16b) is: Find a pair (λ, E) with $\lambda \in \mathbb{C}$ and $E \in H_{\text{curl}}^h(\Omega)$ such that

$$(\nabla \times E, \nabla \times W)_h = \lambda(\varepsilon E, W)_h, \quad \forall W \in H_{\text{curl}}^h(\Omega), \tag{20a}$$

$$(\varepsilon E, \nabla \phi)_h = 0, \quad \forall \phi \in H_{\text{grad}}^h(\Omega). \tag{20b}$$

Here $(f, g)_h$ is a discrete inner product to be specified later.

To simplify the discussion, we only give the details when Ω is a simple cubic (SC) primitive cell with the lattice translation vectors $\mathbf{a}_\ell = a \hat{\mathbf{x}}_\ell$, $\ell = 1, 2, 3$, where $\hat{\mathbf{x}}_\ell$ is the ℓ -th unit vector in \mathbb{R}^3 . Along the way, we also give sufficient remarks for the face-centered cubic (FCC) lattice so that it can be handled similarly. Let h_x, h_y , and h_z be the equal grid spacings along the x, y , and z directions, respectively. Grid points are indexed from 0 to n_i ($i = 1, 2, 3$) with $n_1 = a/h_x, n_2 = a/h_y, n_3 = a/h_z$. Thus the number of the edges parallel to the x -, y - and z -axes, respectively, excluding those on the right, rear, and top surfaces, is just $N = n_1 n_2 n_3$.

From now on, we use $x_m = mh_x$ and $x_{\hat{m}} = \hat{m}h_x$, where $\hat{m} = m + \frac{1}{2}$. Furthermore, for $m = -1, 0, \dots, n_1$, let $\hat{c}_{\hat{m}}(x)$ denote the characteristic function whose value is one over $[x_m, x_{m+1}]$ and zero elsewhere, \hat{l}_i denote the generic global hat function supported over $[x_{i-1}, x_{i+1}]$, i.e., $\hat{l}_i(x_\ell) = \delta_{i\ell}$, for $i = 1, \dots, n_1 - 1$. Here and hereafter, $\delta_{i\ell}$ denotes the Kronecker delta. Similar notations are used for the y and z directions.

We now define piecewise constant functions

$$c_i(x) = \hat{c}_i(x), \quad c_j(y) = \hat{c}_j(y), \quad c_k(z) = \hat{c}_k(z), \tag{21a}$$

for $i \neq 0, n_1 - 1, j \neq 0, n_2 - 1, k \neq 0, n_3 - 1$, and

$$c_0(x) = \hat{c}_0(x) + e^{i2\pi \mathbf{k} \cdot \mathbf{a}_1} \hat{c}_{\hat{n}_1}(x), \quad c_{\hat{n}_1-1}(x) = \hat{c}_{\hat{n}_1-1}(x) + e^{-i2\pi \mathbf{k} \cdot \mathbf{a}_1} \hat{c}_{-\hat{1}}(x), \tag{21b}$$

$$c_0(y) = \hat{c}_0(y) + e^{i2\pi \mathbf{k} \cdot \mathbf{a}_2} \hat{c}_{\hat{n}_2}(y), \quad c_{\hat{n}_2-1}(y) = \hat{c}_{\hat{n}_2-1}(y) + e^{-i2\pi \mathbf{k} \cdot \mathbf{a}_2} \hat{c}_{-\hat{1}}(y), \tag{21c}$$

$$c_0(z) = \hat{c}_0(z) + e^{i2\pi \mathbf{k} \cdot \mathbf{a}_3} \hat{c}_{\hat{n}_3}(z), \quad c_{\hat{n}_3-1}(z) = \hat{c}_{\hat{n}_3-1}(z) + e^{-i2\pi \mathbf{k} \cdot \mathbf{a}_3} \hat{c}_{-\hat{1}}(z), \tag{21d}$$

as well as piecewise linear functions,

$$l_i(x) = \hat{l}_i(x), \quad l_j(y) = \hat{l}_j(y), \quad l_k(z) = \hat{l}_k(z), \tag{22a}$$

for $i, j, k \neq 0$, and

$$l_0(x) = \begin{cases} -h_x^{-1}(x - x_1), & \text{if } x \in [x_0, x_1], \\ e^{i2\pi \mathbf{k} \cdot \mathbf{a}_1} h_x^{-1}(x - x_{n_1-1}), & \text{if } x \in [x_{n_1-1}, x_{n_1}], \\ 0, & \text{otherwise,} \end{cases} \tag{22b}$$

$$l_0(y) = \begin{cases} -h_y^{-1}(y - y_1), & \text{if } y \in [y_0, y_1], \\ e^{i2\pi \mathbf{k} \cdot \mathbf{a}_2} h_y^{-1}(y - y_{n_2-1}), & \text{if } y \in [y_{n_2-1}, y_{n_2}], \\ 0, & \text{otherwise,} \end{cases} \tag{22c}$$

$$l_0(z) = \begin{cases} -h_z^{-1}(z - z_1), & \text{if } z \in [z_0, z_1], \\ e^{i2\pi \mathbf{k} \cdot \mathbf{a}_3} h_z^{-1}(z - z_{n_3-1}), & \text{if } z \in [z_{n_3-1}, z_{n_3}], \\ 0, & \text{otherwise.} \end{cases} \tag{22d}$$

Based on the piecewise constant and linear functions in (21) and (22), we now define bases for the $3N$ -dimensional subspace $H_{\text{curl}}^h(\Omega)$ and N -dimensional subspace $H_{\text{grad}}^h(\Omega)$ in (20), respectively, as

$$H_{\text{curl}}^h(\Omega) = \text{span}\{\phi_1^{i,j,k}\vec{\mathbf{i}}, \phi_2^{r,s,t}\vec{\mathbf{j}}, \phi_3^{\ell,m,n}\vec{\mathbf{k}}\} \subset H_{\text{curl}}(\Omega) \tag{23}$$

and

$$H_{\text{grad}}^h(\Omega) = \text{span}\{\phi^{i,j,k}\} \subset H_{\text{grad}}(\Omega), \tag{24}$$

where $\vec{\mathbf{i}}, \vec{\mathbf{j}}, \vec{\mathbf{k}}$ are the standard unit vectors in \mathbb{R}^3 , and

$$\phi_1^{i,j,k}(x, y, z) := c_i(x)l_j(y)l_k(z), \tag{25a}$$

$$\phi_2^{r,s,t}(x, y, z) := l_r(x)c_s(y)l_t(z), \tag{25b}$$

$$\phi_3^{\ell,m,n}(x, y, z) := l_\ell(x)l_m(y)c_n(z), \tag{25c}$$

$$\phi^{i,j,k}(x, y, z) := l_i(x)l_j(y)l_k(z) \tag{25d}$$

with the sup-indices varying in the set S described as

$$S = \{(i, j, k) : i = 0, \dots, n_1 - 1, j = 0, \dots, n_2 - 1, k = 0, \dots, n_3 - 1\}. \tag{26}$$

The components of an approximate electric field $E \in H_{\text{curl}}^h(\Omega)$ are piecewise constant in one direction and piecewise linear in the other two remaining directions, i.e.,

$$E_1(x, y, z) = \sum_{(i,j,k) \in S} E_1|_{\hat{i},j,k} c_i(x)l_j(y)l_k(z) \equiv \sum_{(i,j,k) \in S} E_1|_{\hat{i},j,k} \phi_1^{i,j,k}, \tag{27a}$$

$$E_2(x, y, z) = \sum_{(i,j,k) \in S} E_2|_{i,\hat{j},k} l_i(x)c_j(y)l_k(z) \equiv \sum_{(i,j,k) \in S} E_2|_{i,\hat{j},k} \phi_2^{i,j,k}, \tag{27b}$$

$$E_3(x, y, z) = \sum_{(i,j,k) \in S} E_3|_{i,j,\hat{k}} l_i(x)l_j(y)c_k(z) \equiv \sum_{(i,j,k) \in S} E_3|_{i,j,\hat{k}} \phi_3^{i,j,k}. \tag{27c}$$

Here in (27a), a subindex (\hat{i}, j, k) indicates that a quantity is located at the midpoint of that edge. By direct evaluation, we see that $E_1|_{\hat{i},j,k} = E_1(x_{i+\frac{1}{2}}, y_j, z_k)$. Similar interpretations hold for E_2 and E_3 . The E_i 's are the familiar edge elements closely related to the finite difference Yee's scheme [9]. In consistent with the quasi-periodic conditions (15), it is easily checked that

$$\text{Left-Right} \begin{cases} E_2|_{n_1,\hat{j},k} = e^{i2\pi\mathbf{k}\cdot\mathbf{a}_1} E_2|_{0,\hat{j},k}, & j = 0 : n_2 - 1, k = 0 : n_3 - 1, \\ E_3|_{n_1,j,\hat{k}} = e^{i2\pi\mathbf{k}\cdot\mathbf{a}_1} E_3|_{0,j,\hat{k}}, & j = 0 : n_2 - 1, k = 0 : n_3 - 1, \end{cases} \tag{28a}$$

$$\text{Front-Rear} \begin{cases} E_1|_{\hat{i},n_2,k} = e^{i2\pi\mathbf{k}\cdot\mathbf{a}_2} E_1|_{\hat{i},0,k}, & i = 0 : n_1 - 1, k = 0 : n_3 - 1, \\ E_3|_{\hat{i},n_2,\hat{k}} = e^{i2\pi\mathbf{k}\cdot\mathbf{a}_2} E_3|_{\hat{i},0,\hat{k}}, & i = 0 : n_1 - 1, k = 0 : n_3 - 1, \end{cases} \tag{28b}$$

$$\text{Top-Bottom} \begin{cases} E_1|_{\hat{i},j,n_3} = e^{i2\pi\mathbf{k}\cdot\mathbf{a}_3} E_1|_{\hat{i},j,0}, & i = 0 : n_1 - 1, j = 0 : n_2 - 1, \\ E_2|_{\hat{i},\hat{j},n_3} = e^{i2\pi\mathbf{k}\cdot\mathbf{a}_3} E_2|_{\hat{i},\hat{j},0}, & i = 0 : n_1 - 1, j = 0 : n_2 - 1. \end{cases} \tag{28c}$$

For the derivation of the generalized eigenvalue problem for (20a), the vectorized form of the discrete electric field E in (27) can be written as

$$\mathbf{e} = [\mathbf{e}_1^\top \quad \mathbf{e}_2^\top \quad \mathbf{e}_3^\top]^\top \tag{29}$$

with

$$\mathbf{e}_1 = \text{vec}\{E_1|_{\hat{i},j,k}\}, \quad \mathbf{e}_2 = \text{vec}\{E_2|_{i,\hat{j},k}\}, \quad \mathbf{e}_3 = \text{vec}\{E_3|_{i,j,\hat{k}}\},$$

for $(i, j, k) \in S$. Here

$$\text{vec}\{F\} := \begin{bmatrix} \text{vec}(F(0 : n_1 - 1, 0 : n_2 - 1, 0)) \\ \text{vec}(F(0 : n_1 - 1, 0 : n_2 - 1, 1)) \\ \vdots \\ \text{vec}(F(0 : n_1 - 1, 0 : n_2 - 1, n_3 - 1)) \end{bmatrix}$$

for given $F \in \mathbb{C}^{n_1 \times n_2 \times n_3}$.

In terms of the basis functions of $H_{\text{curl}}^h(\Omega)$, we expect the discrete weak formulation (20a) to have a matrix form

$$A\mathbf{e} = \lambda B_\varepsilon \mathbf{e}, \tag{30}$$

where \mathbf{e} is as in (29), A and B_ε are matrix representations of the left and right hand sides of (20a), respectively. In Sections 3 and 4, we will use the trapezoidal quadrature

$$\begin{aligned} (f(x), g(x)) &= \int_{x_m}^{x_n} f(x)\overline{g(x)}dx \\ &\approx \frac{h_x}{2} \left[f(x_m)\overline{g(x_m)} + 2 \sum_{i=m+1}^{n-1} f(x_i)\overline{g(x_i)} + f(x_n)\overline{g(x_n)} \right] \\ &\equiv (f(x), g(x))_h \end{aligned} \tag{31}$$

to approximate the discretization in (20a) with $H_{\text{curl}}^h(\Omega)$ in (23) so that the matrix A in (30) is identical to that of Yee's scheme up to a factor $h_x h_y h_z$.

3. Trapezoidal quadrature approximation for $(\nabla \times E, \nabla \times W)$

For a given $E \in H_{\text{curl}}^h(\Omega)$, from (20a) and (23) it suffices to consider the expressions

$$(\nabla \times E, \nabla \times \phi_1^{i,j,k} \vec{\mathbf{i}}), (\nabla \times E, \nabla \times \phi_2^{i,j,k} \vec{\mathbf{j}}), (\nabla \times E, \nabla \times \phi_3^{i,j,k} \vec{\mathbf{k}}) \tag{32}$$

with $(i, j, k) \in S$ in (26) and $\phi_\ell^{i,j,k}$, $\ell = 1, 2, 3$, in (25). In fact, the inner product (\cdot, \cdot) in (32) involves the evaluation of typical terms like (l, c) , (c, l) , (l, l) and (c, c) . For technical derivation, instead of the exact integrals $(l_r(x), l_i(x))$, $(l_s(y), l_j(y))$ and $(l_t(z), l_k(z))$ in (32), we use the trapezoidal quadrature (31) to obtain

$$(l_r(x), l_i(x))_h = \delta_{ri} h_x, \quad (l_s(y), l_j(y))_h = \delta_{sj} h_y, \quad (l_t(z), l_k(z))_h = \delta_{tk} h_z \tag{33}$$

for their approximations.

Let

$$c_{\hat{1}}(x) = e^{i2\pi \mathbf{k} \cdot \mathbf{a}_1} c_{\hat{n}_1-1}(x), \quad c_{\hat{1}}(y) = e^{i2\pi \mathbf{k} \cdot \mathbf{a}_2} c_{\hat{n}_2-1}(y), \quad c_{\hat{1}}(z) = e^{i2\pi \mathbf{k} \cdot \mathbf{a}_3} c_{\hat{n}_3-1}(z). \tag{34}$$

Then the following relations hold:

$$\partial_x l_i(x) = h_x^{-1} (c_{\hat{i}-1}(x) - c_{\hat{i}}(x)), \tag{35a}$$

$$\partial_y l_j(y) = h_y^{-1} (c_{\hat{j}-1}(y) - c_{\hat{j}}(y)), \tag{35b}$$

$$\partial_z l_k(z) = h_z^{-1} (c_{\hat{k}-1}(z) - c_{\hat{k}}(z)), \tag{35c}$$

and

$$\partial_y \phi_1^{i,j,k} = h_y^{-1} c_{\hat{i}} (c_{\hat{j}-1} - c_{\hat{j}}) l_k, \quad \partial_z \phi_1^{i,j,k} = h_z^{-1} c_{\hat{i}} l_j (c_{\hat{k}-1} - c_{\hat{k}}), \tag{36a}$$

$$\partial_x \phi_2^{i,j,k} = h_x^{-1} (c_{\hat{i}-1} - c_{\hat{i}}) c_{\hat{j}} l_k, \quad \partial_z \phi_2^{i,j,k} = h_z^{-1} l_i c_{\hat{j}} (c_{\hat{k}-1} - c_{\hat{k}}), \tag{36b}$$

$$\partial_x \phi_3^{i,j,k} = h_x^{-1} (c_{\hat{i}-1} - c_{\hat{i}}) l_j c_{\hat{k}}, \quad \partial_y \phi_3^{i,j,k} = h_y^{-1} l_i (c_{\hat{j}-1} - c_{\hat{j}}) c_{\hat{k}}, \tag{36c}$$

for $(i, j, k) \in S$.

Before proving the following theorem concerning a certain consistency between our edge element scheme and the finite difference Yee's scheme, we denote the difference matrix with the quasi-periodic condition as

$$K_{n_\ell, \mathbf{a}_\ell} = \begin{bmatrix} 0 & I_{n_\ell-1} \\ e^{i2\pi \mathbf{k} \cdot \mathbf{a}_\ell} & 0 \end{bmatrix} - I_{n_\ell} \in \mathbb{C}^{n_\ell \times n_\ell}, \tag{37}$$

for $\ell = 1, 2, 3$.

Theorem 2. For an SC lattice, the vectorized forms of the inner products described in (32) take on the matrix representation

$$\begin{bmatrix} \text{vec}\{(\nabla \times E, \nabla \times \phi_1^{i,j,k} \vec{\mathbf{i}})_h\}_{(i,j,k) \in S} \\ \text{vec}\{(\nabla \times E, \nabla \times \phi_2^{i,j,k} \vec{\mathbf{j}})_h\}_{(i,j,k) \in S} \\ \text{vec}\{(\nabla \times E, \nabla \times \phi_3^{i,j,k} \vec{\mathbf{k}})_h\}_{(i,j,k) \in S} \end{bmatrix} = (h_x h_y h_z) C^* C \mathbf{e}, \tag{38}$$

where \mathbf{e} is defined in (29),

$$C = \begin{bmatrix} \mathbf{0} & -C_3 & C_2 \\ C_3 & \mathbf{0} & -C_1 \\ -C_2 & C_1 & \mathbf{0} \end{bmatrix} \in \mathbb{C}^{3N \times 3N} \tag{39}$$

with

$$C_1 = h_x^{-1} I_{n_3} \otimes I_{n_2} \otimes K_{n_1, \mathbf{a}_1} \in \mathbb{C}^{N \times N}, \tag{40a}$$

$$C_2 = h_y^{-1} I_{n_3} \otimes K_{n_2, \mathbf{a}_2} \otimes I_{n_1} \in \mathbb{C}^{N \times N}, \tag{40b}$$

$$C_3 = h_z^{-1} K_{n_3, \mathbf{a}_3} \otimes I_{n_2} \otimes I_{n_1} \in \mathbb{C}^{N \times N}, \tag{40c}$$

in which \otimes denotes the Kronecker product.

Proof. We start with the first inner product in (32)

$$(\nabla \times E, \nabla \times \phi_1^{i,j,k} \vec{\mathbf{1}}) = (\partial_z E_1 - \partial_x E_3, \partial_z \phi_1^{i,j,k}) - (\partial_x E_2 - \partial_y E_1, \partial_y \phi_1^{i,j,k}) \tag{41}$$

and the similar process can be applied to the remaining two.

From (27), we have

$$(\partial_z E_1, \partial_z \phi_1^{i,j,k}) = \sum_{(r,s,t) \in S} E_1|_{\hat{r},s,t} (\partial_z \phi_1^{r,s,t}, \partial_z \phi_1^{i,j,k}). \tag{42}$$

It follows from (36) that

$$\begin{aligned} (\partial_z \phi_1^{r,s,t}, \partial_z \phi_1^{i,j,k}) &= h_z^{-2} (c_{\hat{r}} l_s (c_{\hat{r}-1} - c_{\hat{k}}), c_{\hat{i}} l_j (c_{\hat{k}-1} - c_{\hat{k}})) \\ &= h_z^{-2} \int c_{\hat{r}} \bar{c}_{\hat{i}} dx \int l_s \bar{l}_j dy \int (c_{\hat{r}-1} - c_{\hat{i}}) \overline{(c_{\hat{k}-1} - c_{\hat{k}})} dz. \end{aligned} \tag{43}$$

By the definitions of $c_{\hat{i}}(x)$ and $c_{\hat{k}}(z)$ in (21), it holds that

$$(c_{\hat{r}}(x), c_{\hat{i}}(x)) = \delta_{ri} h_x \tag{44}$$

and

$$\begin{aligned} &(c_{\hat{r}-1}(z) - c_{\hat{i}}(z), c_{\hat{k}-1}(z) - c_{\hat{k}}(z)) \\ \stackrel{(34)}{=} &\begin{cases} h_z (-e^{-i2\pi \mathbf{k} \cdot \mathbf{a}_3} \delta_{t,n_3-1} + 2\delta_{t0} - \delta_{t1}), & \text{if } k = 0, \\ h_z (-\delta_{t,k-1} + 2\delta_{tk} - \delta_{t,k+1}), & \text{if } k \neq 0, n_3 - 1, \\ h_z (-\delta_{t,n_3-2} + 2\delta_{t,n_3-1} - e^{i2\pi \mathbf{k} \cdot \mathbf{a}_3} \delta_{t0}), & \text{if } k = n_3 - 1. \end{cases} \end{aligned} \tag{45}$$

Plugging (33), (44) and (45) into (43), we have

$$(\partial_z \phi_1^{r,s,t}, \partial_z \phi_1^{i,j,k})_h = h_z^{-2} (\delta_{ri} h_x) (\delta_{sj} h_y) \times (45).$$

Thus, the inner product in (42) with trapezoidal approximation is equal to

$$\begin{aligned} &h_z (\partial_z E_1, \partial_z \phi_1^{i,j,k})_h \\ &= h_x h_y h_z \frac{-E_1|_{\hat{i},j,k-1} + 2E_1|_{\hat{i},j,k} - E_1|_{\hat{i},j,k+1}}{h_z} \\ &= h_x h_y h_z \left(\frac{E_1|_{\hat{i},j,t+1} - E_1|_{\hat{i},j,t}}{h_z} \Big|_{t=k-1} - \frac{E_1|_{\hat{i},j,t+1} - E_1|_{\hat{i},j,t}}{h_z} \Big|_{t=k} \right) \\ &:= h_x h_y h_z \frac{E_1|_{\hat{i},j,t+1} - E_1|_{\hat{i},j,t}}{h_z} \Big|_{t=k}^{t=k-1} \end{aligned} \tag{46a}$$

by replacing $E_1|_{\hat{i},j,-1}$ and $E_1|_{\hat{i},j,n_3}$ with quasi-periodic conditions

$$E_1|_{\hat{i},j,-1} = e^{-i2\pi \mathbf{k} \cdot \mathbf{a}_3} E_1|_{\hat{i},j,n_3-1} \text{ and } E_1|_{\hat{i},j,n_3} = e^{i2\pi \mathbf{k} \cdot \mathbf{a}_3} E_1|_{\hat{i},j,0},$$

respectively. Similarly,

$$h_y(\partial_y E_1, \partial_y \phi_1^{i,j,k})_h = h_x h_y h_z \frac{E_1|_{\hat{i},s+1,k} - E_1|_{\hat{i},s,k}}{h_y} \Big|_{s=j}^{s=j-1}. \quad (46b)$$

On the other hand, from (27) and (36), we have

$$(\partial_x E_3, \partial_z \phi_1^{i,j,k}) = \sum_{(r,s,t) \in S} E_3|_{r,s,\hat{t}} (\partial_x \phi_3^{r,s,t}, \partial_z \phi_1^{i,j,k}) \quad (47)$$

and

$$\begin{aligned} (\partial_x \phi_3^{r,s,t}, \partial_z \phi_1^{i,j,k}) &= h_x^{-1} h_z^{-1} ((c_{\hat{r}-1} - c_{\hat{r}}) l_s c_{\hat{t}}, c_{\hat{t}}^j l_j (c_{\hat{k}-1} - c_{\hat{k}})) \\ &= h_x^{-1} h_z^{-1} \int (c_{\hat{r}-1} - c_{\hat{r}}) \bar{c}_{\hat{t}} dx \int l_s \bar{l}_j dy \int c_{\hat{t}} (\overline{c_{\hat{k}-1} - c_{\hat{k}}}) dz. \end{aligned} \quad (48)$$

Plugging (33) and

$$\begin{aligned} (c_{\hat{r}-1}(x) - c_{\hat{r}}(x), c_{\hat{t}}(x)) &\stackrel{(34)}{=} \begin{cases} h_x (e^{i2\pi \mathbf{k} \cdot \mathbf{a}_1} \delta_{r,0} - \delta_{r,n_1-1}), & \text{if } i = n_1 - 1, \\ h_x (\delta_{r,i+1} - \delta_{r,i}), & \text{if } i \neq n_1 - 1, \end{cases} \\ (c_{\hat{t}}(z), c_{\hat{k}-1}(z) - c_{\hat{k}}(z)) &\stackrel{(34)}{=} \begin{cases} h_z (e^{-i2\pi \mathbf{k} \cdot \mathbf{a}_3} \delta_{t,n_3-1} - \delta_{t,0}), & \text{if } k = 0, \\ h_z (\delta_{t,k-1} - \delta_{t,k}), & \text{if } k \neq 0 \end{cases} \end{aligned}$$

into (48), the inner product in (47) can be approximated by the trapezoidal rule:

$$\begin{aligned} &(\partial_x E_3, \partial_z \phi_1^{i,j,k})_h \\ &= -h_x h_y h_z \frac{(E_3|_{i+1,j,\hat{k}} - E_3|_{i+1,j,\hat{k}-1}) - (E_3|_{i,j,\hat{k}} - E_3|_{i,j,\hat{k}-1})}{h_x h_z} \\ &= -h_x h_y h_z \frac{E_3|_{r,j,\hat{k}} - E_3|_{r,j,\hat{k}-1}}{h_x h_z} \Big|_{r=i}^{r=i+1} \end{aligned} \quad (49a)$$

by replacing $E_3|_{n_1,j,\hat{k}}$ and $E_3|_{i,j,\hat{-1}}$ with quasi-periodic conditions

$$E_3|_{n_1,j,\hat{k}} = e^{i2\pi \mathbf{k} \cdot \mathbf{a}_3} E_3|_{0,j,\hat{k}} \quad \text{and} \quad E_3|_{i,j,\hat{-1}} = e^{-i2\pi \mathbf{k} \cdot \mathbf{a}_3} E_3|_{i,j,\hat{n}_3-1},$$

respectively. Similarly,

$$\begin{aligned} &(\partial_x E_2, \partial_y \phi_1^{i,j,k})_h \\ &= -h_x h_y h_z \frac{(E_2|_{i+1,\hat{j},k} - E_2|_{i+1,\hat{j}-1,k}) - (E_2|_{i,\hat{j},k} - E_2|_{i,\hat{j}-1,k})}{h_x h_y} \\ &= -h_x h_y h_z \frac{E_2|_{r,\hat{j},k} - E_2|_{r,\hat{j}-1,k}}{h_x h_y} \Big|_{r=i}^{r=i+1} \end{aligned} \quad (49b)$$

From (46) and (49), we see the following central differences:

$$\frac{1}{h_x h_y h_z} (\partial_z E_1, \partial_z \phi_1^{i,j,k})_h = \frac{\partial_z E_1(\hat{i}, \hat{j}, \hat{k} - 1) - \partial_z E_1(\hat{i}, \hat{j}, \hat{k})}{h_z}, \quad (50a)$$

$$\frac{1}{h_x h_y h_z} (\partial_y E_1, \partial_y \phi_1^{i,j,k})_h = \frac{\partial_y E_1(\hat{i}, \hat{j} - 1, k) - \partial_y E_1(\hat{i}, \hat{j}, k)}{h_y}, \quad (50b)$$

$$\frac{1}{h_x h_y h_z} (\partial_x E_3, \partial_z \phi_1^{i,j,k})_h = \frac{\partial_z E_3(i+1, j, k) - \partial_z E_3(i, j, k)}{h_x}, \quad (50c)$$

$$\frac{1}{h_x h_y h_z} (\partial_x E_2, \partial_y \phi_1^{i,j,k})_h = \frac{\partial_y E_2(i+1, j, k) - \partial_y E_2(i, j, k)}{h_x}. \quad (50d)$$

Then, letting $H = \nabla \times E$, it is now not hard to see from (41) and (50) that

$$\begin{aligned} & \frac{1}{h_x h_y h_z} \left(\nabla \times E, \nabla \times \phi_1^{i,j,k} \vec{\mathbf{i}} \right)_h \\ &= \frac{H_2(\hat{i}, j, \hat{k} - 1) - H_2(\hat{i}, j, \hat{k})}{h_z} - \frac{H_3(\hat{i}, \hat{j} - 1, k) - H_3(\hat{i}, \hat{j}, k)}{h_y} \\ &= -\partial_z H_2(\hat{i}, j, k) + \partial_y H_3(\hat{i}, j, k) \\ &= (\nabla \times H)_1(\hat{i}, j, k). \end{aligned}$$

Similarly, we have

$$\begin{aligned} & \frac{1}{h_x h_y h_z} \left(\nabla \times E, \nabla \times \phi_2^{i,j,k} \vec{\mathbf{j}} \right)_h = (\nabla \times H)_2(i, \hat{j}, k), \\ & \frac{1}{h_x h_y h_z} \left(\nabla \times E, \nabla \times \phi_3^{i,j,k} \vec{\mathbf{k}} \right)_h = (\nabla \times H)_3(i, j, \hat{k}). \end{aligned}$$

This shows that the edge element method with the trapezoidal rule and the finite difference Yee’s scheme produce the same left-hand side up to a factor. On the other hand, from the results in [8], the matrix form of the discrete double curl operator by using Yee’s scheme is C^*C . Consequently, the vectorized forms of the inner products in (32) have the form of (38). □

Remark 5. The quasi-periodic condition is easily enforced for the approximate electric field E in the SC lattice since the lattice translation vectors $\mathbf{a}_\ell = a\hat{\mathbf{x}}_\ell$. For the FCC lattice they are not aligned with the coordinator axes, we must derive the non-diagonal relations, for example, the top-bottom variables are not componentwise related as above. The relations are already derived in [15].

Remark 6. For a FCC lattice, the matrices $C_1, C_2,$ and C_3 with quasi-periodic condition (4) are somewhat complicated which can be found in Appendix.

From Theorem 2, the edge elements allow the traditional Yee’s discretization done for $\nabla \times (\nabla \times \mathbb{E})$ to be preserved. The edge finite element method (20a) with the trapezoidal rule is equivalent to the finite difference Yee’s scheme up to a factor of $h_x h_y h_z$. That is, edge elements and Yee’s discretization generate the discrete matrices $h_x h_y h_z A$ and A , respectively, where A is of the form

$$A = C^*C, \tag{51}$$

and has the following eigen-decomposition.

Theorem 3 ([8,14]). Let $C_\ell, \ell = 1, 2, 3$ and A be defined in (40) and (51), respectively. Then C_1, C_2, C_3 are simultaneously diagonalizable by unitary matrix $T \in \mathbb{C}^{n \times n}$ in the forms

$$C_\ell T = T \Lambda_\ell, \quad \ell = 1, 2, 3, \tag{52}$$

where Λ_ℓ is the eigenvalue matrix for C_ℓ . Moreover, there is an orthonormal matrix

$$Q_r := (I_3 \otimes T) \Pi_r \equiv (I_3 \otimes T) \begin{bmatrix} \Pi_{r,1} & \Pi_{r,2} \\ \Pi_{r,3} & \Pi_{r,4} \\ \Pi_{r,5} & \Pi_{r,6} \end{bmatrix} \in \mathbb{C}^{3N \times 2N}, \tag{53}$$

where $\Pi_{r,j} \in \mathbb{C}^{N \times N}, j = 1, \dots, 6,$ are diagonal such that A has an eigen-decomposition of the form

$$Q_r^* A Q_r = \text{diag}(\Lambda_q, \Lambda_q) \equiv \Lambda_r$$

with Λ_q being a diagonal matrix whose diagonal entries are the positive eigenvalues of A .

4. Trapezoidal quadrature approximation for $(\epsilon E, W)$

In this section, we will derive the discretization of the right-hand side of (20a). For simplicity, let $\epsilon_{rs}^{i,j,k}$ denote the value of ϵ_{rs} at the point (ih_x, jh_y, kh_z) , for $r, s = 1, 2, 3$. Recalling the basis for $H_{\text{curl}}^h(\Omega)$ defined in (23), we consider

$$(\epsilon E, \phi_1^{i,j,k} \vec{\mathbf{i}}), (\epsilon E, \phi_2^{i,j,k} \vec{\mathbf{j}}), (\epsilon E, \phi_3^{i,j,k} \vec{\mathbf{k}}) \tag{54}$$

with sup-indices (i, j, k) in S and discuss the componentwise contributions resulted from applying the trapezoidal rule in (31) to the integrals on the right-hand side of (20a).

To this end, we first give a useful lemma.

Lemma 1. Let $f : \mathbb{R} \rightarrow \mathbb{C}$ be a piecewise constant function defined on $[x_0, x_{n_1}]$ satisfying the periodic boundary condition $f(x_0) = f(x_{n_1})$. Then, for given $r, i = 0, 1, \dots, n_1 - 1$, we have trapezoidal approximations

$$(f c_{\hat{r}}, c_{\hat{i}})_h = \frac{h_x}{2} (\delta_{r,i-1} f(x_i) + \delta_{ri} (f(x_i) + f(x_{i+1})) + \delta_{r,i+1} f(x_{i+1})), \quad (55a)$$

$$(f l_r, l_i)_h = h_x \delta_{ri} f(x_i), \quad (55b)$$

$$(f c_{\hat{r}}, l_i)_h = \frac{h_x}{2} \begin{cases} (\delta_{r,i-1} + \delta_{ri}) f(x_i), & \text{if } i \neq 0, \\ (\delta_{r0} + e^{-i2\pi \mathbf{k} \cdot \mathbf{a}_1} \delta_{r,n_1-1}) f(x_0), & \text{if } i = 0, \end{cases} \quad (55c)$$

$$(f l_r, c_{\hat{i}})_h = \frac{h_x}{2} \begin{cases} \delta_{ri} f(x_i) + \delta_{r,i+1} f(x_{i+1}), & \text{if } i \neq n_1 - 1, \\ e^{i2\pi \mathbf{k} \cdot \mathbf{a}_1} \delta_{r0} f(x_0) + \delta_{r,n_1-1} f(x_{n_1-1}), & \text{if } i = n_1 - 1. \end{cases} \quad (55d)$$

Similar relations hold for the y - and z -directions.

Proof. From the definitions of $c_{\hat{i}}(x)$ in (21) and $l_i(x)$ in (22), it holds that

$$\begin{aligned} (f c_{\hat{r}}, c_{\hat{i}}) &= \int_{x_0}^{x_{n_1}} f(x) c_{\hat{r}}(x) \overline{c_{\hat{i}}(x)} dx = \int_{x_i}^{x_{i+1}} f(x) c_{\hat{r}}(x) dx, \\ (f l_r, l_i) &= \int_{x_0}^{x_{n_1}} f(x) l_r(x) \overline{l_i(x)} dx = \int_{x_{i-1}}^{x_{i+1}} f(x) l_r(x) \overline{l_i(x)} dx, \\ (f c_{\hat{r}}, l_i) &= \int_{x_0}^{x_{n_1}} f(x) c_{\hat{r}}(x) \overline{l_i(x)} dx = \int_{x_r}^{x_{r+1}} f(x) \overline{l_i(x)} dx, \\ (f l_r, c_{\hat{i}}) &= \int_{x_0}^{x_{n_1}} f(x) l_r(x) \overline{c_{\hat{i}}(x)} dx = \int_{x_i}^{x_{i+1}} f(x) l_r(x) dx. \end{aligned}$$

Then, using the trapezoidal rule in (31) directly, we obtain

$$\begin{aligned} (f c_{\hat{r}}, c_{\hat{i}})_h &= \frac{h_x}{2} ((f c_{\hat{r}})(x_i) + (f c_{\hat{r}})(x_{i+1})) \\ &= \frac{h_x}{2} (\delta_{r,i-1} f(x_i) + \delta_{ri} (f(x_i) + f(x_{i+1})) + \delta_{r,i+1} f(x_{i+1})), \\ (f l_r, l_i)_h &= h_x \frac{(f l_r \overline{l_i})(x_{i-1}) + 2(f l_r \overline{l_i})(x_i) + (f l_r \overline{l_i})(x_{i+1}))}{2} = h_x \delta_{ri} f(x_i), \end{aligned}$$

and

$$\begin{aligned} (f c_{\hat{r}}, l_i)_h &= h_x \frac{(f \overline{l_i})(x_r) + (f \overline{l_i})(x_{r+1}))}{2} \\ &= \begin{cases} h_x \frac{(\delta_{ri} + \delta_{r,i-1}) f(x_i)}{2}, & \text{if } i \neq 0, \\ h_x \frac{(\delta_{r0} + e^{-i2\pi \mathbf{k} \cdot \mathbf{a}_1} \delta_{r,n_1-1}) f(x_0)}{2}, & \text{if } i = 0, \end{cases} \\ (f l_r, c_{\hat{i}})_h &= h_x \frac{(f l_r)(x_i) + (f l_r)(x_{i+1}))}{2} \\ &= \begin{cases} h_x \frac{(\delta_{ri} f(x_i) + \delta_{r,i+1} f(x_{i+1}))}{2}, & \text{if } i \neq n_1 - 1, \\ h_x \frac{(e^{i2\pi \mathbf{k} \cdot \mathbf{a}_1} \delta_{r0} f(x_0) + \delta_{r,n_1-1} f(x_{n_1-1}))}{2}, & \text{if } i = n_1 - 1. \quad \square \end{cases} \end{aligned}$$

4.1. Trapezoidal approximation for diagonal entries

The diagonal entries of inner products in (54) are considered as

$$(\varepsilon_{mm} E_m, \phi_m^{i,j,k}), \quad \text{for } m = 1, 2, 3. \quad (56)$$

From (55a)-(55b) in Lemma 1, we have

$$\begin{aligned}
 & (\varepsilon_{11}\phi_1^{r,s,t}, \phi_1^{i,j,k})_h \\
 = & h_x h_y h_z \delta_{sj} \delta_{tk} \frac{\delta_{r,i-1} \varepsilon_{11}^{i,j,k} + \delta_{ri} (\varepsilon_{11}^{i,j,k} + \varepsilon_{11}^{i+1,j,k}) + \delta_{r,i+1} \varepsilon_{11}^{i+1,j,k}}{2},
 \end{aligned} \tag{57a}$$

$$\begin{aligned}
 & (\varepsilon_{22}\phi_2^{r,s,t}, \phi_2^{i,j,k})_h \\
 = & h_x h_y h_z \delta_{ri} \delta_{tk} \frac{\delta_{s,j-1} \varepsilon_{22}^{i,j,k} + \delta_{sj} (\varepsilon_{22}^{i,j,k} + \varepsilon_{22}^{i,j+1,k}) + \delta_{s,j+1} \varepsilon_{22}^{i,j+1,k}}{2},
 \end{aligned} \tag{57b}$$

$$\begin{aligned}
 & (\varepsilon_{33}\phi_3^{r,s,t}, \phi_3^{i,j,k})_h \\
 = & h_x h_y h_z \delta_{ri} \delta_{sj} \frac{\delta_{t,k-1} \varepsilon_{33}^{i,j,k} + \delta_{tk} (\varepsilon_{33}^{i,j,k} + \varepsilon_{33}^{i,j,k+1}) + \delta_{t,k+1} \varepsilon_{33}^{i,j,k+1}}{2}.
 \end{aligned} \tag{57c}$$

Then, by evaluating the Kronecker delta in (57) carefully, the inner products in (56) have matrix representations as

$$\begin{aligned}
 & \text{vec}\{(\varepsilon_{mm} E_m, \phi_m^{i,j,k})_h\}_{(i,j,k) \in S} \\
 = & \frac{h_x h_y h_z}{2} (D_{\varepsilon_{mm}} (h_\alpha C_m + 2I)^* + D_{\varepsilon'_{mm}} (h_\alpha C_m + 2I)) \mathbf{e}_m.
 \end{aligned} \tag{58}$$

Here α can be subscripts x, y, z of the grid spacings h_x, h_y and h_z , respectively, corresponding to $m = 1, 2, 3$ and $D_{\varepsilon_{mm}}, D_{\varepsilon'_{mm}}$ are diagonal matrices, in general, given by

$$D_{\varepsilon_{mn}} = \text{diag}\{\varepsilon_{mn}(x_i, y_j, z_k)\}_{(i,j,k) \in S}, \tag{59a}$$

$$D_{\varepsilon'_{1n}} = \text{diag}\{\varepsilon_{1n}(x_{i+1}, y_j, z_k)\}_{(i,j,k) \in S}, \tag{59b}$$

$$D_{\varepsilon'_{2n}} = \text{diag}\{\varepsilon_{2n}(x_i, y_{j+1}, z_k)\}_{(i,j,k) \in S}, \tag{59c}$$

$$D_{\varepsilon'_{3n}} = \text{diag}\{\varepsilon_{3n}(x_i, y_j, z_{k+1})\}_{(i,j,k) \in S}, \tag{59d}$$

for $m, n = 1, 2, 3$. Here $\text{diag}\{F\} := \text{diag}(\text{vec}\{F\})$ for any $F \in \mathbb{C}^{n_1 \times n_2 \times n_3}$.

4.2. Trapezoidal approximation for off-diagonal entries

The off-diagonal entries of inner products in (54) are considered as

$$(\varepsilon_{mn} E_n, \phi_m^{i,j,k}), \quad \text{for } m, n = 1, 2, 3, m \neq n.$$

From (55c)-(55d) in Lemma 1, we have

$$\begin{aligned}
 & (\varepsilon_{12}\phi_2^{r,s,t}, \phi_1^{i,j,k})_h = \\
 & \frac{h_x h_y h_z}{4} \begin{cases} \delta_{tk} (\delta_{s,j-1} + \delta_{sj}) (\delta_{ri} \varepsilon_{12}^{i,j,k} + \delta_{r,i+1} \varepsilon_{12}^{i+1,j,k}), & \text{if } j \neq 0, i \neq n_1 - 1, \\ \delta_{tk} (\delta_{s0} + e^{-i2\pi \mathbf{k} \cdot \mathbf{a}_2} \delta_{s,n_2-1}) (\delta_{ri} \varepsilon_{12}^{i,0,k} + \delta_{r,i+1} \varepsilon_{12}^{i+1,0,k}), & \text{if } j = 0, i \neq n_1 - 1, \\ \delta_{tk} (\delta_{s,j-1} + \delta_{sj}) (e^{i2\pi \mathbf{k} \cdot \mathbf{a}_1} \delta_{r0} \varepsilon_{12}^{0,j,k} + \delta_{r,n_1-1} \varepsilon_{12}^{n_1-1,j,k}), & \text{if } j \neq 0, i = n_1 - 1, \\ \delta_{tk} (\delta_{s0} + e^{-i2\pi \mathbf{k} \cdot \mathbf{a}_2} \delta_{s,n_2-1}) (e^{i2\pi \mathbf{k} \cdot \mathbf{a}_1} \delta_{r0} \varepsilon_{12}^{0,0,k} + \delta_{r,n_1-1} \varepsilon_{12}^{n_1-1,0,k}), & \text{if } j = 0, i = n_1 - 1, \end{cases}
 \end{aligned} \tag{60}$$

and

$$\begin{aligned}
 & (\varepsilon_{21}\phi_1^{r,s,t}, \phi_2^{i,j,k})_h = \\
 & \frac{h_x h_y h_z}{4} \begin{cases} \delta_{tk} (\delta_{r,i-1} + \delta_{ri}) (\delta_{sj} \varepsilon_{21}^{i,j,k} + \delta_{s,j+1} \varepsilon_{21}^{i,j+1,k}), & \text{if } i \neq 0, j \neq n_2 - 1, \\ \delta_{tk} (\delta_{r0} + e^{-i2\pi \mathbf{k} \cdot \mathbf{a}_1} \delta_{r,n_1-1}) (\delta_{sj} \varepsilon_{21}^{0,j,k} + \delta_{s,j+1} \varepsilon_{21}^{0,j+1,k}), & \text{if } i = 0, j \neq n_2 - 1, \\ \delta_{tk} (\delta_{r,i-1} + \delta_{ri}) (e^{i2\pi \mathbf{k} \cdot \mathbf{a}_2} \delta_{s0} \varepsilon_{21}^{i,0,k} + \delta_{s,n_2-1} \varepsilon_{21}^{i,n_2-1,k}), & \text{if } i \neq 0, j = n_2 - 1, \\ \delta_{tk} (\delta_{r0} + e^{-i2\pi \mathbf{k} \cdot \mathbf{a}_1} \delta_{r,n_1-1}) (e^{i2\pi \mathbf{k} \cdot \mathbf{a}_2} \delta_{s0} \varepsilon_{21}^{0,0,k} + \delta_{s,n_2-1} \varepsilon_{21}^{0,n_2-1,k}), & \text{if } i = 0, j = n_2 - 1. \end{cases}
 \end{aligned} \tag{61}$$

Furthermore, these inner products have matrix representations as

$$\begin{aligned} \text{vec}\{(\varepsilon_{12}E_2, \phi_1^{i,j,k})_h\}_{(i,j,k)\in S} &= \frac{h_x h_y h_z}{4} \left[D_{\varepsilon_{12}}(h_y C_2 + 2I)^* + D_{\varepsilon'_{12}}(h_y C_2 + 2I)^*(h_x C_1 + I) \right] \mathbf{e}_2, \\ \text{vec}\{(\varepsilon_{21}E_1, \phi_2^{i,j,k})_h\}_{(i,j,k)\in S} &= \frac{h_x h_y h_z}{4} \left[D_{\varepsilon_{21}}(h_x C_1 + 2I)^* + D_{\varepsilon'_{21}}(h_x C_1 + 2I)^*(h_y C_2 + I) \right] \mathbf{e}_1, \end{aligned}$$

where $D_{\varepsilon_{mn}}$ and $D_{\varepsilon'_{mn}}$ are defined in (59).

By the same process as above, we conclude that

$$\begin{aligned} &\text{vec}\{(\varepsilon_{mn}E_n, \phi_m^{i,j,k})_h\}_{(i,j,k)\in S} \\ &= \frac{h_x h_y h_z}{4} \left[D_{\varepsilon_{mn}}(h_\beta C_n + 2I)^* + D_{\varepsilon'_{mn}}(h_\beta C_n + 2I)^*(h_\alpha C_m + I) \right] \mathbf{e}_n, \end{aligned} \tag{62}$$

where $(\alpha, \beta) = (x, y), (y, x), (y, z), (z, y), (z, x), (x, z)$ corresponding to $(m, n) = (1, 2), (2, 1), (2, 3), (3, 2), (3, 1), (1, 3)$, respectively.

Finally, from (58) and (62), the right-hand side of (20a) can be discretized as the matrix form

$$h_x h_y h_z B_\varepsilon \mathbf{e} \equiv \frac{h_x h_y h_z}{4} \begin{bmatrix} 2B_{11} & B_{12} & B_{13} \\ B_{21} & 2B_{22} & B_{23} \\ B_{31} & B_{32} & 2B_{33} \end{bmatrix} \begin{bmatrix} \mathbf{e}_1 \\ \mathbf{e}_2 \\ \mathbf{e}_3 \end{bmatrix}, \tag{63}$$

where

$$B_{mm} = D_{\varepsilon_{mn}}(h_\alpha C_m + 2I)^* + D_{\varepsilon'_{mn}}(h_\alpha C_m + 2I) \tag{64a}$$

and

$$B_{mn} = D_{\varepsilon_{mn}}(h_\beta C_n + 2I)^* + D_{\varepsilon'_{mn}}(h_\beta C_n + 2I)^*(h_\alpha C_m + I) \tag{64b}$$

in which $(\alpha, \beta) = (x, y), (y, x), (y, z), (z, y), (z, x), (x, z)$ corresponding to $(m, n) = (1, 2), (2, 1), (2, 3), (3, 2), (3, 1), (1, 3)$.

Remark 7. In the previous section we showed that the left side of the edge finite element method (20a) with the trapezoidal rule is equivalent to finite difference Yee’s scheme up to a factor of $h_x h_y h_z$. Notice that all coefficients above have the same factor as well. Consequently, our finite element method can be interpreted as a finite difference method once we combine Yee’s scheme with our right-hand side discretization divided by $h_x h_y h_z$.

5. Null-space free method and divergence-free condition

The matrix representation B_ε of the discretization in terms of the discrete electric field $\mathbf{e} = [\mathbf{e}_1^\top \ \mathbf{e}_2^\top \ \mathbf{e}_3^\top]^\top$ from the right-hand side of (20a) can be written as in (63). Now, we give a lemma for the matrix factorizations of $D_{\varepsilon'_{mn}}$ and B_{mn} in (59b)-(59d) and (64), respectively.

Lemma 2. The matrices in (59b)-(59d) can be written as

$$D_{\varepsilon'_{1n}} = (h_x C_1 + I)D_{\varepsilon_{1n}}(h_x C_1 + I)^*, \tag{65a}$$

$$D_{\varepsilon'_{2n}} = (h_y C_2 + I)D_{\varepsilon_{2n}}(h_y C_2 + I)^*, \tag{65b}$$

$$D_{\varepsilon'_{3n}} = (h_z C_3 + I)D_{\varepsilon_{3n}}(h_z C_3 + I)^*, \tag{65c}$$

and, for the matrices B_{mn} in (64), $m, n = 1, 2, 3$, we have

$$B_{mn} = (h_\alpha C_m + 2I)D_{\varepsilon_{mn}}(h_\beta C_n + 2I)^*. \tag{66}$$

Here α and β can be subscripts x, y, z of the grid spacings h_x, h_y and h_z , respectively, corresponding to $m, n = 1, 2, 3$.

Proof. First, we show that (65a) holds and the similar process can be applied for (65b) and (65c). From the Kronecker product and the periodicity of ε_{1n} , it apparently holds that

$$\text{diag}(\varepsilon_{1n}(1 : n_1, j, k)) = (K_{n_1, \mathbf{a}_1} + I)\text{diag}(\varepsilon_{1n}(0 : n_1 - 1, j, k))(K_{n_1, \mathbf{a}_1} + I)^*$$

for $j = 0, \dots, n_2 - 1, k = 0, \dots, n_3 - 1$, where K_{n_1, \mathbf{a}_1} is defined in (37).

Next, for (66), by plugging (65a)-(65c) into (64a) and (64b), respectively, we get

$$\begin{aligned} B_{mm} &= D_{\varepsilon_{mm}}(h_\alpha C_m + 2I)^* + D_{\varepsilon'_{mm}}(h_\alpha C_m + 2I) \\ &= D_{\varepsilon_{mm}}(h_\alpha C_m + 2I)^* + (h_\alpha C_m + I)D_{\varepsilon_{mm}}(h_\alpha C_m + I)^*(h_\alpha C_m + 2I) \\ &= D_{\varepsilon_{mm}}(h_\alpha C_m + 2I)^* + (h_\alpha C_m + I)D_{\varepsilon_{mm}}(h_\alpha C_m + 2I)^* \\ &= (h_\alpha C_m + 2I)D_{\varepsilon_{mm}}(h_\alpha C_m + 2I)^* \end{aligned}$$

and

$$\begin{aligned} B_{mn} &= D_{\varepsilon_{mn}}(h_\beta C_n + 2I)^* + D_{\varepsilon'_{mn}}(h_\beta C_n + 2I)^*(h_\alpha C_m + I) \\ &= [D_{\varepsilon_{mn}} + (h_\alpha C_m + I)D_{\varepsilon_{mn}}(h_\alpha C_m + I)^*(h_\alpha C_m + I)](h_\beta C_n + 2I)^* \\ &= (h_\alpha C_m + 2I)D_{\varepsilon_{mn}}(h_\beta C_n + 2I)^*, \end{aligned}$$

for $m \neq n$. □

The HPD property of B_ε can be shown immediately by using Lemma 2.

Theorem 4. The matrix B_ε in (63) is HPD, if the tensor field ε in (17) is also HPD. In fact, B_ε can be written as the matrix representation

$$B_\varepsilon = \frac{1}{4} P D_\varepsilon P^* \tag{67}$$

where

$$P = \begin{bmatrix} h_x C_1 + 2I & & \\ & h_y C_2 + 2I & \\ & & h_z C_3 + 2I \end{bmatrix}, \quad D_\varepsilon = \begin{bmatrix} 2D_{\varepsilon_{11}} & D_{\varepsilon_{12}} & D_{\varepsilon_{13}} \\ D_{\varepsilon_{21}} & 2D_{\varepsilon_{22}} & D_{\varepsilon_{23}} \\ D_{\varepsilon_{31}} & D_{\varepsilon_{32}} & 2D_{\varepsilon_{33}} \end{bmatrix}. \tag{68}$$

Proof. The matrix factorization in (67) can be derived from (66). If ε is HPD, then D_ε in (68) is also HPD and therefore, B_ε is HPD. □

In the original finite difference Yee's scheme, there is no need to compute E_ℓ , $\ell = 1, 2, 3$, on the edges orthogonal to x -, y -, z -axis, respectively. That is fine if ε is a scalar field, but when ε is a matrix, the E_ℓ will also appear on the edges orthogonal to the $\hat{\mathbf{x}}_\ell$ direction via the product εE and a naive extension of the finite difference Yee's scheme using the averages will give rise to a nonsymmetric B_ε in (30). Thus, it is possible for such a scheme to produce complex eigenvalues instead of just the (correct) real eigenvalues, which is incorrect if ε is positive definite.

So in the context of a finite difference scheme, the right side of Galerkin finite element formulation (20a) actually provides the right weights. This gives our method a more natural interpretation as a modified finite difference Yee's scheme, which seems to be more intuitive for people working in the field of computational electromagnetics. Furthermore, the special factorization (67) of the HPD matrix B_ε results in minimal effort in inverting B_ε while still keeping the correct physics intact (real frequencies).

5.1. The null-space free method

From (51) and Theorem 4, we have that all eigenvalues of the resulting GEP (30) are real if the tensor field ε is Hermitian. Moreover, these eigenvalues are non-negative if ε is HPD. By Theorem 3, the GEP (30) can be transformed to a null-space free standard eigenvalue problem (NFSEP)

$$\left(\Lambda_r^{\frac{1}{2}} Q_r^* B_\varepsilon^{-1} Q_r \Lambda_r^{\frac{1}{2}} \right) \mathbf{y} = \lambda \mathbf{y}. \tag{69}$$

Both of the GEP and the corresponding NFSEP have the same positive eigenvalues, while the zero eigenvalues of the GEP are deflated [14,16]. Because $\Lambda_r^{\frac{1}{2}} Q_r^* B_\varepsilon^{-1} Q_r \Lambda_r^{\frac{1}{2}}$ is Hermitian, we can use the invert Lanczos method to find some smallest target eigenvalues of (69). In each iteration of the invert Lanczos method, we need to solve the linear system

$$\left(\Lambda_r^{1/2} Q_r^* B_\varepsilon^{-1} Q_r \Lambda_r^{1/2} \right) \mathbf{z} = \mathbf{d}$$

or equivalently

$$(Q_r^* B_\varepsilon^{-1} Q_r) \tilde{\mathbf{z}} = \Lambda_r^{-1/2} \mathbf{d}, \quad \mathbf{z} = \Lambda_r^{-1/2} \tilde{\mathbf{z}} \tag{70}$$

for a given vector \mathbf{d} .

Plugging the results in (52) into (68), the matrix P can be factored as

$$P = (I_3 \otimes T) \begin{bmatrix} h_x \Lambda_1 + 2I & & \\ & h_y \Lambda_2 + 2I & \\ & & h_z \Lambda_3 + 2I \end{bmatrix} (I_3 \otimes T)^* \\ \equiv (I_3 \otimes T) D_\Lambda (I_3 \otimes T)^*,$$

which implies that

$$B_\varepsilon = \frac{1}{4} (I_3 \otimes T) D_\Lambda (I_3 \otimes T)^* D_\varepsilon (I_3 \otimes T) D_\Lambda^* (I_3 \otimes T)^*.$$

From (53), we have

$$Q_r^* B_\varepsilon^{-1} Q_r = 4 \Pi_r^* D_\Lambda^{-*} (I_3 \otimes T^*) D_\varepsilon^{-1} (I_3 \otimes T) D_\Lambda^{-1} \Pi_r. \tag{71}$$

Since D_ε in (68) is a 3×3 block diagonal matrix after a suitable permutation, the most computationally expensive part of solving the linear system with coefficient matrix (71) is the computation of the matrix-vector multiplications $T\mathbf{q}$ and $T^*\mathbf{p}$. Remarkably, these two multiplications can be efficiently computed by the developed FFT-based methods in [8,14] without explicitly forming the matrix T .

5.2. Divergence free condition

We now show the discrete divergence free condition (20b) holds, i.e.,

$$(\varepsilon E, \nabla \phi^{i,j,k})_h = 0, \quad \forall (i, j, k) \in S, \tag{72}$$

where $\phi^{i,j,k} \in H_{\text{grad}}^h(\Omega)$ is defined in (25). By (35)-(36), we have

$$\partial_x \phi^{i,j,k} = \begin{cases} h_x^{-1} (\phi_1^{i-1,j,k} - \phi_1^{i,j,k}), & \text{if } i \neq 0, \\ h_x^{-1} (e^{i2\pi \mathbf{k} \cdot \mathbf{a}_1} \phi_1^{n_1-1,j,k} - \phi_1^{0,j,k}), & \text{if } i = 0, \end{cases} \tag{73a}$$

$$\partial_y \phi^{i,j,k} = \begin{cases} h_y^{-1} (\phi_2^{i,j-1,k} - \phi_2^{i,j,k}), & \text{if } j \neq 0, \\ h_y^{-1} (e^{i2\pi \mathbf{k} \cdot \mathbf{a}_2} \phi_2^{i,n_2-1,k} - \phi_2^{i,0,k}), & \text{if } j = 0, \end{cases} \tag{73b}$$

$$\partial_z \phi^{i,j,k} = \begin{cases} h_z^{-1} (\phi_3^{i,j,k-1} - \phi_3^{i,j,k}), & \text{if } k \neq 0, \\ h_z^{-1} (e^{i2\pi \mathbf{k} \cdot \mathbf{a}_3} \phi_3^{i,j,n_3-1} - \phi_3^{i,j,0}), & \text{if } k = 0, \end{cases} \tag{73c}$$

and hence

$$\nabla \left(H_{\text{grad}}^h(\Omega) \right) \subset H_{\text{curl}}^h(\Omega). \tag{74}$$

This together with (20a) shows that (20b) holds, when $\lambda \neq 0$. Alternatively, substituting (73) into (72) and using $(\varepsilon E, \phi_1^{i,j,k} \vec{\mathbf{i}})_h$, $(\varepsilon E, \phi_2^{i,j,k} \vec{\mathbf{j}})_h$ and $(\varepsilon E, \phi_3^{i,j,k} \vec{\mathbf{k}})_h$ in Section 4, we see that Eq. (72) holds if and only if

$$N_c^* B_\varepsilon \mathbf{e} \equiv [C_1^* \quad C_2^* \quad C_3^*] B_\varepsilon \mathbf{e} = 0. \tag{75}$$

Theorem 5. Let (λ, \mathbf{y}) be an eigenpair of NFSEP (69) and define

$$\mathbf{e} = B_\varepsilon^{-1} Q_r \Lambda_r^{1/2} \mathbf{y}.$$

Then (λ, \mathbf{e}) is an eigenpair of GEP (30) and \mathbf{e} automatically satisfies the divergence free condition (75).

Proof. As shown in [14] and Theorem 3, the columns of N_c and Q_r , respectively, span the invariant subspaces of the Hermitian matrix A corresponding to zero and nonzero eigenvalues. This implies that if $B_\varepsilon \mathbf{e} \in \text{span}\{Q_r\}$, then (75) is automatically satisfied. Moreover, from the result in [14], the columns of $B_\varepsilon^{-1} Q_r$ spans the invariant subspace of the GEP (30) corresponding to nonzero eigenvalues. The invariant subspace $\text{span}\{B_\varepsilon^{-1} Q_r\}$ is then applied to reduce GEP (30) into NFSEP (69) with $\mathbf{e} = B_\varepsilon^{-1} Q_r \Lambda_r^{1/2} \mathbf{y}$. This means that such eigenvector \mathbf{e} automatically satisfies the divergence free condition (75). \square

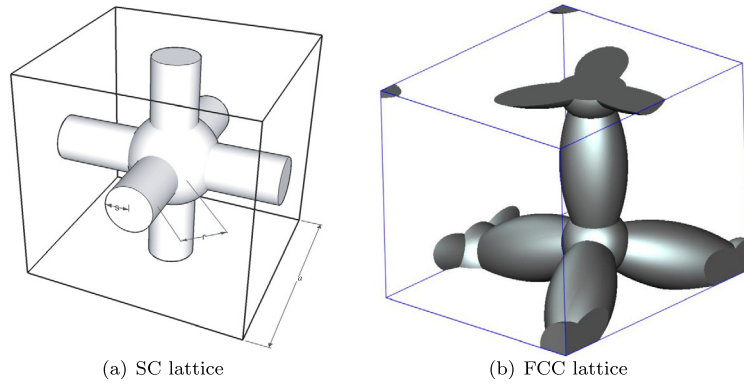


Fig. 1. Schema of 3D anisotropic medium with SC and FCC lattices within a single primitive cell.

6. Numerical experiments

To study the convergence behavior of the eigensolvers in terms of iteration numbers, we consider the SC and FCC lattices described in [8,14].

For the SC lattice, we consider a lattice consisting of spheres with radius r and circular cylinders with radius s , as shown in Fig. 1(a). In particular, we assume the lattice constant $a = 1$, $r/a = 0.345$, and $s/a = 0.11$. The perimeter of the irreducible Brillouin zone for the SC lattice is formed by the corners $G = [0, 0, 0]^T$, $X = \frac{2\pi}{a} [\frac{1}{2}, 0, 0]^T$, $M = \frac{2\pi}{a} [\frac{1}{2}, \frac{1}{2}, 0]^T$, and $R = \frac{2\pi}{a} [\frac{1}{2}, \frac{1}{2}, \frac{1}{2}]^T$.

For the FCC lattice, we consider a lattice consisting of dielectric spheres with a connecting cylinder as shown in Fig. 1(b). The radius r of the spheres is $r = 0.12a$ and the connecting cylinder has a radius $s = 0.11a$. The perimeter of the irreducible Brillouin zone for the lattice is formed by the corners $X = \frac{2\pi}{a} \Phi [0, 1, 0]^T$, $U = \frac{2\pi}{a} \Phi [\frac{1}{4}, 1, \frac{1}{4}]^T$, $L = \frac{2\pi}{a} \Phi [\frac{1}{2}, \frac{1}{2}, \frac{1}{2}]^T$, $G = [0, 0, 0]^T$, $W = \frac{2\pi}{a} \Phi [\frac{1}{2}, 1, 0]^T$, and $K = \frac{2\pi}{a} \Phi [\frac{3}{4}, \frac{3}{4}, 0]^T$, where

$$\Phi = \frac{1}{\sqrt{2}} \begin{bmatrix} 1 & 1 & 0 \\ -\frac{1}{\sqrt{3}} & \frac{1}{\sqrt{3}} & \frac{2}{\sqrt{3}} \\ \frac{2}{\sqrt{6}} & -\frac{2}{\sqrt{6}} & \frac{2}{\sqrt{6}} \end{bmatrix}.$$

All computations in this section are carried out in MATLAB 2017a, and the MATLAB functions `fft` and `ifft` are applied to compute the matrix-vector multiplications $T^* \mathbf{p}$ and $T \mathbf{q}$, respectively.

The SC and FCC anisotropic media have the permittivity tensors $\epsilon_s(\mathbf{x})$ and $\epsilon_f(\mathbf{x})$ [27,28], respectively, where $\epsilon_s(\mathbf{x})$ and $\epsilon_f(\mathbf{x})$ are defined as

$$\epsilon_s(\mathbf{x}) = \begin{bmatrix} \epsilon_{11}(\mathbf{x}) & 0 & -i\epsilon_{13}(\mathbf{x}) \\ 0 & \epsilon_{22}(\mathbf{x}) & 0 \\ i\epsilon_{13}(\mathbf{x}) & 0 & \epsilon_{11}(\mathbf{x}) \end{bmatrix}, \quad \epsilon_f(\mathbf{x}) = \Phi \epsilon_s(\mathbf{x}) \Phi^T \tag{76}$$

at position $\mathbf{x} \in \mathbb{R}^3$. Here

$$\begin{aligned} \epsilon_{11} &= \begin{cases} \sqrt{1 + |\beta|^2} \epsilon, & \text{if } \mathbf{x} \text{ in the anisotropic medium,} \\ 1, & \text{otherwise,} \end{cases} \\ \epsilon_{22} &= \begin{cases} \epsilon, & \text{if } \mathbf{x} \text{ in the anisotropic medium,} \\ 1, & \text{otherwise,} \end{cases} \\ \epsilon_{13} &= \begin{cases} |\beta| \epsilon, & \text{if } \mathbf{x} \text{ in the anisotropic medium,} \\ 1, & \text{otherwise,} \end{cases} \end{aligned}$$

with external magnetic field intensity β . It is clear that

$$\det(\epsilon_s(\mathbf{x})) = \det(\epsilon_f(\mathbf{x})) = \epsilon^3$$

if \mathbf{x} is in the material. We take $\epsilon = 13$ and $|\beta| = 0.875$ in the following discussion.

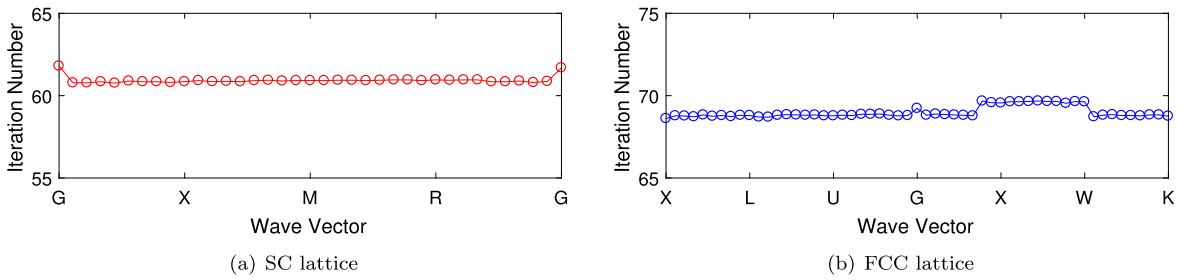


Fig. 2. Iteration numbers of the CG method for solving $Q_r^* B_\epsilon^{-1} Q_r \mathbf{z} = \mathbf{d}$ with the external magnetic field intensity $|\beta| = 0.875$ and the matrix dimension $3n = 3 \times 120^3 = 5,184,000$.

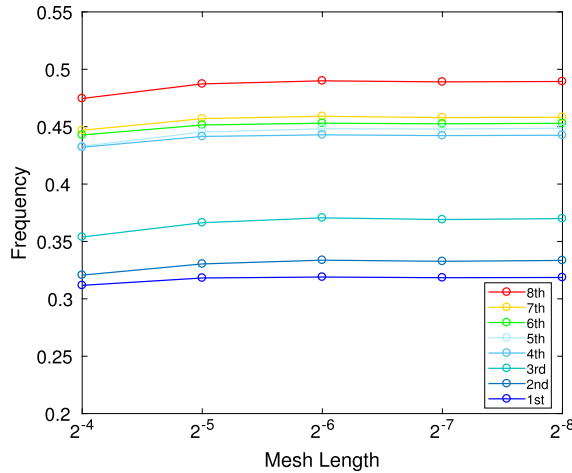


Fig. 3. The convergence of the smallest target eigenvalues for the NFSEP (69) with SC lattice. Various coarse mesh lengths are used. (For interpretation of the colors in the figure(s), the reader is referred to the web version of this article.)

6.1. Performance of solving linear systems

Based on the above prescribed permittivity tensors ϵ_s and ϵ_f of (76), we know that the coefficient matrix B_ϵ in (67) is also HPD, and the associated linear system is easily solved. Therefore, we can apply the CG method without preconditioning to solve the linear system $Q_r^* B_\epsilon^{-1} Q_r \mathbf{z} = \mathbf{d}$ in each iteration of the eigensolver for NFSEP (69). Using a stopping tolerance of 10^{-12} , the associated iteration numbers with various wave vectors are shown in Fig. 2. They range in the vicinities of 63 and 69 iterations for the SC and FCC lattices, respectively.

6.2. Convergence and performance of eigensolver

First, we illustrate convergence of the eigenvalues. Since the coefficient matrix $\Lambda_r^{\frac{1}{2}} Q_r^* B_\epsilon^{-1} Q_r \Lambda_r^{\frac{1}{2}}$ in (69) is HPD, the invert Lanczos method is applied to compute the smallest target eigenvalues of (69). For the SC lattice and the wave vector $\mathbf{k} = [0.5, 0.5, 0.06]$, we set mesh lengths $h_x = h_y = h_z = h$. The computed eigenvalues of (69) with $h = 2^{-4}, 2^{-5}, 2^{-6}, 2^{-7}$ and 2^{-8} are shown in Fig. 3, which indicates convergence to the right frequency in all cases considered.

Taking $|\beta| = 0.875$ and $n_1 = n_2 = n_3 = 120$, the computed band structures of SC and FCC lattices are demonstrated in Fig. 4. For each wave vector \mathbf{k} in Fig. 4, the total iteration numbers it takes for the invert Lanczos method to solve (69) for the eight smallest target eigenvalues are shown in Fig. 5. Among all cases tested for solving each of the target eigenvalues, the invert Lanczos method takes 45 to 55 iterations (46.7 on average) for the SC lattice, 46 to 60 iterations (53.2 on average) for the FCC lattice. These small iteration numbers for such large problems are indeed remarkable.

7. Conclusions

In this paper, we have shown that our finite element method can be interpreted as a modified finite difference Yee’s scheme for the following reasons: (i) For the left-hand side of (1), through the discrete inner products with trapezoidal quadratures, we derived the discrete double curl operator A , which coincides with the finite difference Yee’s scheme C^*C up to a factor $h_x h_y h_z$. Therefore, the well-known eigen-decomposition of C^*C can be applied. (ii) For the right-hand side of (1), we derived an HPD-preserving coefficient matrix B_ϵ , i.e., if ϵ is HPD, so is B_ϵ . In contrast, the coefficient matrix

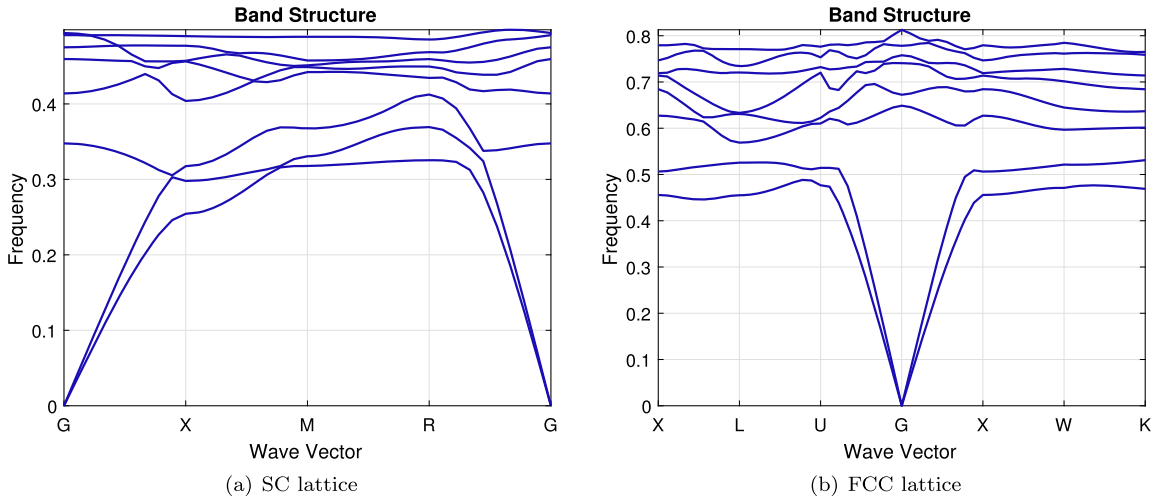


Fig. 4. Computed band structures of SC and FCC lattices with the external magnetic field intensity $|\beta| = 0.875$ and the matrix dimension $3n = 3 \times 120^3 = 5,184,000$.

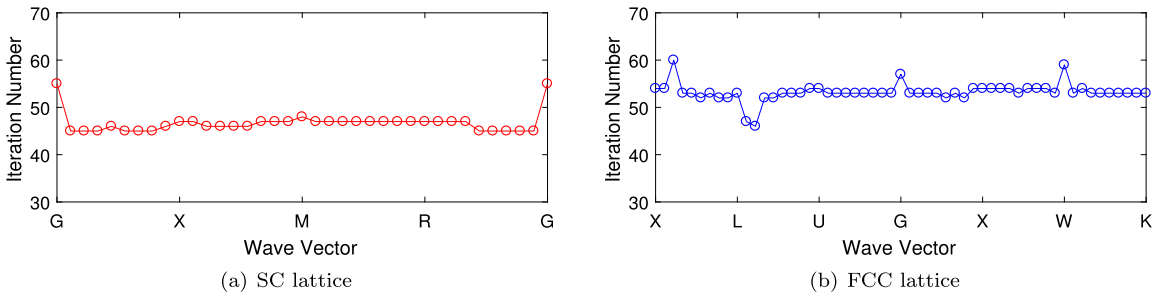


Fig. 5. Iteration numbers of the invert Lanczos method with various wave vector $2\pi\mathbf{k}$. Here external magnetic field intensity $|\beta| = 0.875$ and matrix dimension $3n = 3 \times 120^3 = 5,184,000$.

B_ε generated by Yee’s scheme does not enjoy this property. Furthermore, the matrix B_ε can be factorized by FFT-matrices and a 3×3 block diagonal matrix with a suitable permutation. Thus, the linear system for B_ε can be easily solved. In conclusion, the NFSEP can then be solved by the invert Lanczos method and the linear system at each iteration step can be efficiently solved by the CG method without any preconditioner. Numerical results show the effectiveness of our proposed finite element method.

Acknowledgements

The authors thank the anonymous referees for their useful comments and suggestions. Chou’s summer visit was partially supported by the National Center for Theoretical Sciences (NCTS) and the ST. Yau Center, Hsinchu, Taiwan. Huang was partially supported by the Ministry of Science and Technology (MOST) 105-2115-M-003-009-MY3, and NCTS in Taiwan. Li was supported in parts by the NSFC 11471074. Lin was partially supported by MOST 106-2628-M-009-004, NCTS, and ST Yau Center.

Appendix

Define

$$K_{m,\mathbf{a}} = \begin{bmatrix} 0 & I_{m-1} \\ e^{i2\pi\mathbf{k}\cdot\mathbf{a}} & 0 \end{bmatrix} - I_m \in \mathbb{C}^{m \times m}.$$

Then, for the SC lattice [8], the discrete partial derivative operators in (40) can be written as

$$C_1 = h_x^{-1} I_{n_3} \otimes I_{n_2} \otimes K_1, \quad C_2 = h_y^{-1} I_{n_3} \otimes K_2, \quad C_3 = h_z^{-1} K_3,$$

where

$$K_1 = K_{n_1,\mathbf{a}_1}, \quad K_2 = K_{n_2,\mathbf{a}_2} \otimes I_{n_1}, \quad K_3 = K_{n_3,\mathbf{a}_3} \otimes I_{n_2} \otimes I_{n_1};$$

for the face-centered cubic (FCC) lattice [14], they are

$$K_1 = K_{n_1, \mathbf{a}_1}, \quad K_2 = K_{n_2, \mathbf{a}_1, \mathbf{a}_2} \equiv \begin{bmatrix} 0 & I_{n_1(n_2-1)} \\ e^{i2\pi \mathbf{k} \cdot \mathbf{a}_2} J_{2, \mathbf{a}_1} & 0 \end{bmatrix} - I_{n_1 n_2},$$

$$K_3 = K_{n_3, \mathbf{a}_1, \mathbf{a}_2, \mathbf{a}_3} \equiv \begin{bmatrix} 0 & I_{n_1 n_2 (n_3-1)} \\ e^{i2\pi \mathbf{k} \cdot \mathbf{a}_3} J_{3, \mathbf{a}_1, \mathbf{a}_2} & 0 \end{bmatrix} - I_{n_1 n_2 n_3},$$

where

$$J_{2, \mathbf{a}_1} = \begin{bmatrix} 0 & e^{-i2\pi \mathbf{k} \cdot \mathbf{a}_1} I_{n_1/2} \\ I_{n_1/2} & 0 \end{bmatrix},$$

$$J_{3, \mathbf{a}_1, \mathbf{a}_2} = \begin{bmatrix} 0 & e^{-i2\pi \mathbf{k} \cdot \mathbf{a}_2} I_{\frac{1}{3}n_2} \otimes I_{n_1} \\ I_{\frac{2}{3}n_2} \otimes J_{2, \mathbf{a}_1} & 0 \end{bmatrix}$$

and

$$\mathbf{a}_1 = \frac{a}{\sqrt{2}} [1, 0, 0]^T, \quad \mathbf{a}_2 = \frac{a}{\sqrt{2}} \left[\frac{1}{2}, \frac{\sqrt{3}}{2}, 0 \right]^T, \quad \text{and} \quad \mathbf{a}_3 = \frac{a}{\sqrt{2}} \left[\frac{1}{2}, \frac{1}{2\sqrt{3}}, \sqrt{\frac{2}{3}} \right]^T,$$

in which a is a lattice constant.

References

- [1] G. Bao, P. Li, H. Wu, An adaptive edge element method with perfectly matched absorbing layers for wave scattering by bi-periodic structures, *Math. Comput.* 79 (2010) 1–34.
- [2] A. Bjarklev, J. Broeng, A.S. Bjarklev, Fabrication of photonic crystal fibres, in: *Photonic Crystal Fibres*, Springer, 2003, pp. 115–130.
- [3] D. Boffi, Finite element approximations of eigenvalue problems, *Acta Numer.* 19 (2010) 1.
- [4] D. Boffi, M. Conforti, L. Gastaldi, Modified edge finite elements for photonic crystals, *Numer. Math.* 105 (2006) 249–266.
- [5] A. Bossavit, Mixed finite elements and the complex of Whitney forms, in: *The Mathematics of Finite Elements and Applications VI*, Academic Press, San Diego, CA, 1988, pp. 137–144.
- [6] F. Bréchet, J. Marcou, D. Pagnoux, P. Roy, Complete analysis of the characteristics of propagation into photonic crystal fibers, by the finite element method, *Opt. Fiber Technol.* 6 (2000) 181–191.
- [7] K. Busch, S. John, Liquid-crystal photonic-band-gap materials: the tunable electromagnetic vacuum, *Phys. Rev. Lett.* 83 (1999) 967–970.
- [8] R.-L. Chern, H.-E. Hsieh, T.-M. Huang, W.-W. Lin, W. Wang, Singular value decompositions for single-curl operators in three-dimensional Maxwell's equations for complex media, *SIAM J. Matrix Anal. Appl.* 36 (2015) 203–224.
- [9] S.H. Chou, W.-W. Lin, Eigendecompositions and fast eigensolvers for Maxwell equations, *Not. ICCM* 4 (2016) 46–54.
- [10] D.C. Dobson, An efficient method for band structure calculations in 2D photonic crystals, *J. Comput. Phys.* 149 (1999) 363–376.
- [11] W. Dörfler, A. Lechleiter, M. Plum, G. Schneider, C. Wieners, *Photonic Crystals: Mathematical Analysis and Numerical Approximation*, Springer, Basel AG, 2011.
- [12] V. Girault, P.A. Raviart, *Finite Element Methods for Navier-Stokes Equations: Theory and Algorithms*, Springer-Verlag, 1986.
- [13] S. Guo, F. Wu, S. Albin, R.S. Rogowski, Photonic band gap analysis using finite-difference frequency-domain method, *Opt. Express* 12 (2004) 1741–1746.
- [14] T.-M. Huang, H.-E. Hsieh, W.-W. Lin, W. Wang, Eigendecomposition of the discrete double-curl operator with application to fast eigensolver for three dimensional photonic crystals, *SIAM J. Matrix Anal. Appl.* 34 (2013) 369–391.
- [15] T.-M. Huang, H.-E. Hsieh, W.-W. Lin, W. Wang, Matrix representation of the double-curl operator for simulating three dimensional photonic crystals, *Math. Comput. Model.* 58 (2013) 379–392.
- [16] T.-M. Huang, H.-E. Hsieh, W.-W. Lin, W. Wang, Eigenvalue solvers for three dimensional photonic crystals with face-centered cubic lattice, *J. Comput. Appl. Math.* 272 (2014) 350–361.
- [17] T.-M. Huang, T. Li, R.-L. Chern, W.-W. Lin, Electromagnetic field behavior of 3D Maxwell's equations for chiral media, *J. Comput. Phys.* 379 (2019) 118–131, <https://doi.org/10.1016/j.jcp.2018.11.026>.
- [18] T.-M. Huang, W.-W. Lin, V. Mehrmann, A Newton-type method with nonequivalence deflation for nonlinear eigenvalue problems arising in photonic crystal modeling, *SIAM J. Sci. Comput.* 38 (2016) B191–B218.
- [19] J.M. Hyman, M. Shashkov, Mimetic discretizations of Maxwell's equations, *J. Comput. Phys.* 151 (1999) 881–909.
- [20] J.M. Jarem, P.P. Banerjee, *Computational Methods for Electromagnetic and Optical Systems*, CRC Press, 2011.
- [21] W. Jiang, N. Liu, Y. Yue, Q.H. Liu, Mixed finite-element method for resonant cavity problem with complex geometric topology and anisotropic lossless media, *IEEE Trans. Magn.* 52 (2016) 7400108.
- [22] F. Karaomerlioglu, S. Simsek, A.M. Mamedov, E. Ozbay, 2D Anisotropic Photonic Crystals of Hollow Semiconductor Nanorod with Liquid Crystals, *Applied Mechanics and Materials*, vol. 394, Trans Tech Publ, 2013, pp. 38–44.
- [23] Z.Y. Li, J. Wang, B.Y. Gu, Creation of partial band gaps in anisotropic photonic-band-gap structures, *Phys. Rev. B* 58 (1998) 3721–3729.
- [24] Z.Y. Li, J. Wang, B.Y. Gu, Large absolute band gap in 2D anisotropic photonic crystals, *Phys. Rev. Lett.* 81 (1998) 2574–2577.
- [25] N. Liu, G. Cai, C. Zhu, Y. Huang, Q.H. Liu, The mixed finite-element method with mass lumping for computing optical waveguide modes, *IEEE J. Sel. Top. Quantum Electron.* 22 (2016) 4400709.
- [26] N. Liu, L.E. Tobón, Y. Zhao, Y. Tang, Q.H. Liu, Mixed spectral-element method for 3-D Maxwell's eigenvalue problem, *IEEE Trans. Microw. Theory Tech.* 63 (2015) 317–325.
- [27] L.-Z. Lu, C. Fang, L. Fu, S.G. Johnson, J.D. Joannopoulos, M. Soljačić, Symmetry-protected topological photonic crystal in three dimensions, *Nat. Phys.* 12 (2016) 337–340.
- [28] L.-Z. Lu, L. Fu, J.D. Joannopoulos, M. Soljačić, Weyl points and line nodes in gyroid photonic crystals, *Nat. Photonics* 7 (2013) 294–299.
- [29] M. Luo, Q.H. Liu, Accurate determination of band structures of two-dimensional dispersive anisotropic photonic crystals by the spectral element method, *J. Opt. Soc. Am. A* 26 (7) (2009) 1598–1605.
- [30] M. Luo, Q.H. Liu, Z. Li, Spectral element method for band structures of two-dimensional anisotropic photonic crystals, *Phys. Rev. E* 79 (2009) 026705.

- [31] P. Monk, *Finite Element Methods for Maxwell's Equations*, Oxford University Press, Oxford, UK, 2003.
- [32] J.-C. Nédélec, Mixed finite elements in \mathbb{R}^3 , *Numer. Math.* 35 (1980) 315–341.
- [33] J.-C. Nédélec, A new class of mixed finite elements in \mathbb{R}^3 , *Numer. Math.* 50 (1986) 57–81.
- [34] R.A. Nicolaides, D.-Q. Wang, Convergence analysis of a covolume scheme for Maxwell's equations in three dimensions, *Math. Comput.* 67 (1998) 947–963.
- [35] M. Richter, *Optimization of Photonic Band Structures*, PhD thesis, Karlsruhe Institute of Technology, 2010.
- [36] R.C. Rumpf, C.R. Garcia, E.A. Berry, J.H. Barton, Finite-difference frequency-domain algorithm for modeling electromagnetic scattering from general anisotropic objects, *Prog. Electromagn. Res. B* 61 (2014) 55–67.
- [37] K. Saitoh, M. Koshiba, Full-vectorial imaginary-distance beam propagation method based on a finite element scheme: application to photonic crystal fibers, *IEEE J. Quantum Electron.* 7 (2002) 927–933.
- [38] H.-B. Sun, V. Mizeikis, Y. Xu, S. Juodkazis, J.-Y. Ye, S. Matsuo, H. Misawa, Microcavities in polymeric photonic crystals, *Appl. Phys. Lett.* 79 (2001) 1–3.
- [39] H. Whitney, *Geometric Integration Theory*, Princeton Univ. Press, Princeton, NJ, 1957.
- [40] K. Yee, Numerical solution of initial boundary value problems involving Maxwell's equations in isotropic media, *IEEE Trans. Antennas Propag.* 14 (1966) 302–307.
- [41] I.H.H. Zabel, D. Stroud, Photonic band structures of optically anisotropic periodic arrays, *Phys. Rev. B* 48 (1993) 5004–5012.